TKP4580 - Specialization Project, Process Systems Engineering

Dynamic modeling and control of a system of electrolyzers for hydrogen production

Md Rizwan

Submission date: 19.12.2019
Supervisors: Johannes Jaschke, IKP
Vidar Alstad, Yara International ASA
Sarmad Munir, Yara International ASA

NTNU
Norwegian University of
Science and Technology
Department of Chemical Engineering

Dedicated to my parents

Summary

In the efforts to reduce greenhouse gas emissions and the dependence on fossil fuel based energy sources, hydrogen based technologies involving development of the large scale water electrolysis plant offers one of the most promising solutions for the future energy economy. The aim of this project is to develop a mathematical model for an alkaline water electrolyzer plant and then use it to study operational performance of the plant under variable power scenarios.
A simplified model for the electrolyzer plant consisting of four sub domains i.e. electrolyzer assembly, lye circulation system, compressor and the gas storage system was developed using systems approach. Empirical correlations are used to define the involved overvoltages in the electrolyzer. However, dynamic response analysis revealed the instabilities present within the developed model. The root cause of this behavior was assessed to be the mismatch between the net heat generated and overall heat taken out form the electrolyzer system.
The design of a regulatory control layer is proposed to stabilize the electrolyzer plant. This control layer removes the open loop feedback responses that are drifting away the process towards instability. The simple proportional controller manipulates the cooling duty in the lye circulation loop Q_{cool} to maintain the inlet lye temperature T_{in} to its desired set-point value. However, implementation of remaining controllers in the regulatory layer and the selection of set-point trajectory for regulatory layer is the subject of the supervisory layer control design which is planned to be included in the future work on this project.

Preface

This report is written for TKP4580 Chemical engineering, specialization project at Norwegian University of Science and Technology (NTNU). The work presented here in this report was conducted during Autumn 2019 as a collaboration project between NTNU and Yara International ASA.
Working on this project has been an extremely satisfying experience, as it involves the application of process system engineering concepts to study the solutions for a real world problem. First of all, I would like to thank NTNU and Yara International ASA for offering me the possibility to work on this project. I would also extend deep appreciation towards my supervisor, Johannes Jaschke and co-supervisors, Vidar Alstad and Sarmad Munir from Yara International ASA for the support and encouragement throughout the course of this project. I am profoundly indebted to them for sharing their knowledge and experience with me. Their commitment and adherence to high standards has enabled me to finally come up with this final research document, that I am proud to present here.

Table of Contents

List of Figures

List of Symbols

Symbol	Definition	Unit
A	Area	m^2
I	Current	A
emf	Electromotive force	V
U	Cell voltage	V
ΔG	Change in gibbs energy	$Jmol^{-1}$
ΔH	Change in enthalpy	$Jmol^{-1}$
ΔG	Change in entropy	$JK^{-1}mol^{-1}$
r_1	parameter related to ohmic resistance of electrolyzer	Ωm^2
r_2	parameter related to ohmic resistance of electrolyzer	Ωm^2 °C^{-1}
s	coefficient for overvoltage on electrodes	V
t_1	coefficient for overvoltage on electrodes	m^2 A^{-1}
t_2	coefficient for overvoltage on electrodes	m^2 A^{-1}°C
t_3	coefficient for overvoltage on electrodes	m^2 A^{-1}°C^2
η_F	Faraday efficiency	
η_e	Energy efficiency	
f_1	parameter related to Faraday efficiency	mA^2cm^{-4}
f_2	parameter related to Faraday efficiency	
$\dot{n}$	molar flow rate	mol/s
n_c	number of cells in series per stack	
C_t	overall thermal capacity of the electrolyzer	JK^{-1}
R_t	overall thermal resistance of the electrolyzer	$W^{-1}K$
$\dot{Q}$	heat transfer rate	W
T	Temperature	K or °C
τ_t	thermal time constant	s
k	Polytropic exponent	
γ	Adiabatic exponent	
α	Compressor efficiency	
w	Polytropic work	$Jmol^{-1}$
E_p	Polytropic efficiency	
k_{vlv}	valve constant	mol/(s.$\sqrt{bar}$)
z	Valve displacement	
Constants		
z	Number of electrons transferred per reaction	2
F	Faraday constant	96485

Chapter 1

Introduction

This chapter gives background of this project report. Scope of this study for the modeling and control of alkaline water electrolyzer plant is introduced and previous work done for the modeling of electrolyzer is described. Furthermore, main structure of the report is explained.

1.1 Background

Ammonia is one of the basic chemicals to produce nitrogenous fertilizers. Approximately 88% of ammonia [16] produced globally is used to manufacture inorganic fertilizers which are crucial for feeding the planet.
Industrially, ammonia is produced via the Haber Bosch process which requires hydrogen and nitrogen in the ratio 3:1 at moderately elevated temperature (450 °C) and high pressure (100+ bar).

$$\mathrm{N_2} + 3\,\mathrm{H_2} \longrightarrow 2\,\mathrm{NH_3} \tag{1.1}$$

The nitrogen is extracted from air and hydrogen is currently obtained by steam-methane reforming of natural gas. The consumption of fossil energy for ammonia production is essential to produce fertilizer and contributes to around 1.5% of the world greenhouse gas emissions [10]. The fertilizer industry is cognizant of the critical importance to reduce this dependence on natural gas and reduce GHG emissions. Therefore, the ways of obtaining hydrogen from carbon free sources should be explored to make fertilizer production more sustainable and greener.

1.2 Green Fertilizer Production

Green fertilizer production refers to the production of fertilizers from sustainable sources. This technology explore ways to produce hydrogen without using fossil fuels.
Water electrolysis using renewable power to generate hydrogen is the most promising option that will help to eliminate the dependence on fossil fuel-based sources. The main

water electrolysis technologies present today are alkaline water electrolysis (AEL), proton exchange membrane electrolysis (PEMEL) and solid oxide electrolysis (SOEL). Out of these, Alkaline water electrolysis (AEL) is the most mature and commercially available electrolysis technology [4]. It has been around for over a century and that is why the first step in making fertilizer industry greener could be to make the production of hydrogen from alkaline water electrolysis industrially profitable.

1.3 Technology: Alkaline Water Electrolysis

Electrolysis is the decomposition of water into hydrogen and oxygen by passing an electric current (DC) between two electrodes separated by an aqueous electrolyte with good ionic conductivity. In an alkaline electrolyzer, the electrolyte is usually aqueous potassium hydroxide (KOH), where the potassium ion K^+ and hydroxide ion OH take care of the ionic transport. The anodic and cathodic reactions taking place here are

$$Anode : 2\,OH^- \text{ (aq)} \longrightarrow \frac{1}{2}\,\mathrm{O_2\,(g)} + \mathrm{H_2O\ (l)} + 2\,e^- \tag{1.2}$$

$$Cathode : 2\,\mathrm{H_2O\ (l)} + 2\,e^- \longrightarrow \mathrm{H_2\,(g)} + 2\,OH^-\ \text{(aq)} \tag{1.3}$$

Operating temperature is set mainly between 70-100 °C and operating pressure is between 1 and 30 bars.[19]
The electrodes are immersed in an alkaline aqueous solution with weight concentration (20-30 wt.%) and therefore they must be corrosion resistant, have good electrical conductivity and catalytic properties, allowing better electrochemical transfer. Physically an

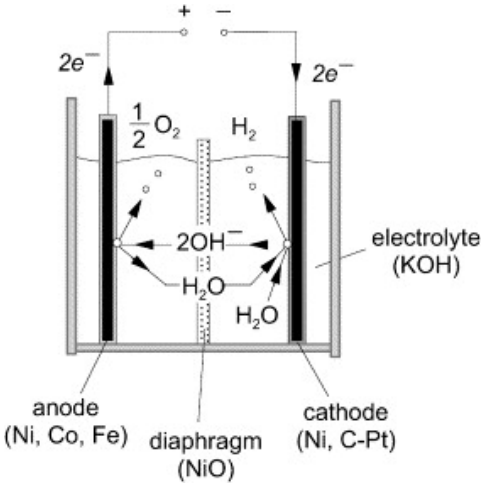

Figure 1.1: Schematic of the alkaline electrolyzer cell [19]

electrolyzer consists of several cells. There are two electrolysis cell configurations based on how these cells are connected namely, monopolar and bipolar cell configuration.

In monopolar configuration, each cell is connected in parallel to form large module of electrolysis stack. Hence, the voltage between individual pair of cells is directly equal to the total cell voltage and the sum of cell current is equal to the total cell current. In this configuration, diaphragm separates the anodic and cathodic sections and the electrode is located in each section. Therefore, same electrochemical reaction (reduction/oxidation) occurs on both sides of each electrode.

In bipolar design, each cell is connected in series to form large module of electrolysis

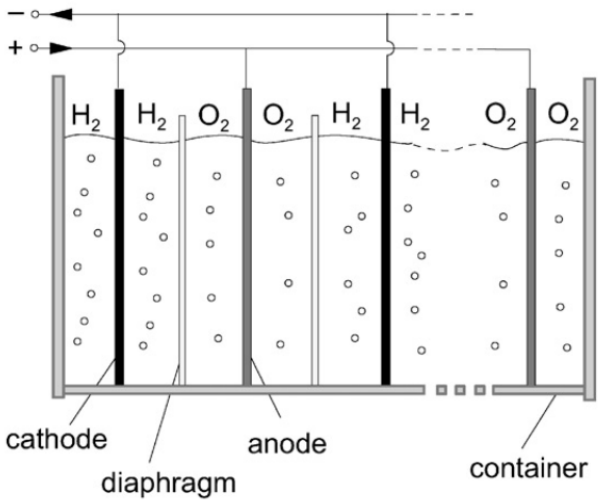

Figure 1.2: Principle of monopolar electrolyzer design [19]

stack. Hence, the cell current is directly equal to the current which is passed through each individual cell and the sum of voltages between individual pairs is equal to the total cell voltage. Bipolar plate separate individual cells in this configuration. This bipolar plate acts as anode for one cell and as cathode for the other cell. Therefore, two different electrochemical reaction occurs on both sides of each bipolar plate. Most commercial alkaline electrolyzers today are bipolar as they are more compact, gives shorter current paths in electrical wires and electrodes and has better electrolyzer efficiency. However, there are also some disadvantages with the bipolar designs like, parasitic currents which are generated in the cell because of movement of the ions in the migration electric field and can cause corrosion problems.

In the case of atmospheric electrolyzers, a compressor unit is required to increase the pressure before storing the hydrogen produced. Operation at higher pressure would overcome the compression step and increase overall efficiency. Electrolyzers operated at either atmospheric pressure or at the pressure up to 30 bar represent the current state of the art with regard to the product gas pressure.

Here we have discussed the standalone operation of alkaline electrolyzers and we disregard any coupling to the power source (like one in [15] where direct coupling of alkaline electrolyser cell and PV module is discussed).

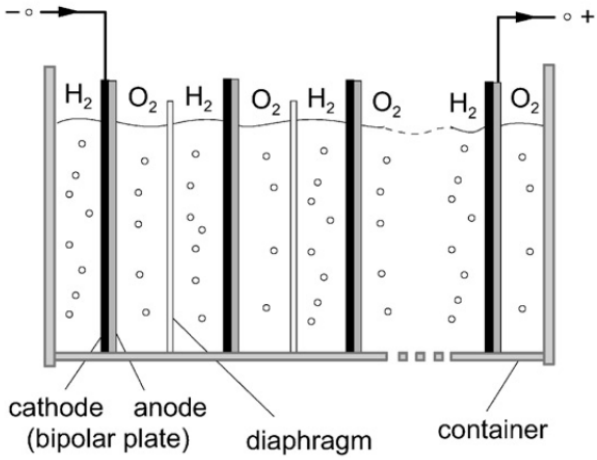

Figure 1.3: Principle of bipolar electrolyzer design [19]

1.4 Scope of Work

Using systems approach this project aims to develop mathematical model of an alkaline water electrolyzer plant to explore possible application of automatic control for dynamic operation of this plant in variable power scenario.
This study assumes usage of renewable power sources to provide electricity for electrolysis. These sources are intermittent in nature and that is why the model developed should be robust to predict all the system properties. The developed mathematical model is implemented in MATLAB using CasADi symbolic framework [1]. The model is solved using the numerical integrator IDAS, available in open-source software SUNDIALS suite, and simulation of different scenarios for operation of this dynamic system of electrolyzers will be performed. The main goal is to suggest a control structure that can ensure flexibility of the alkaline water electrolyzer plant with respect to input power variations.

1.5 Previous Work

There are different approaches to the dynamic modelling of alkaline electrolyzers. The model by Ulleberg [19] is based on a combination of fundamental thermodynamics, heat transfer theory, and empirical electrochemical relationships. This model predicts the cell voltage, hydrogen production, efficiencies, and operating temperature and is the most widely used model in the literature for dynamic modelling of alkaline electrolyzers.
Prior to this, the most relevant electrolyzer model from 1990s was SIMELINT-program developed by Bussmann et.al. [9]. This program which was validated against measured data, accurately predicts the thermal behaviour, cell voltage, gas purities, and efficiencies for any given power or current profile.
The model developed by Ulleberg [19] requires experimental data to be collected over

couple of weeks to correctly estimate the parameters for empirical correlations. Therefore, efforts have been made in recent years by Hammoudi et.al. [6] to develop a multi-physics model for the design and diagnosis of the alkaline electrolyzers. The approach allows the characterization of the electrolyzer based on its structural parameters in a relatively short time (few minutes). The model considers the variation of all structural parameters (geometry, materials and their evolution depending on operating conditions) and operational parameters of the electrolyzer (temperature, pressure, concentration, bulk bubbling and recovery rate of electrode surface by the bubble), while the model by Ulleberg [19] involve only the temperature.
In continuation to the work presented in [6], C. Henao et al. have proposed an Alkaline Electrolyser Simulation Tool (AEST) [8] based on a physics model with an electrical analogy in order to emulate the physical and electrical behaviour of the alkaline electrolyser. This paper discusses the power electronics involved in alkaline electrolyzer and simulation results using MATLAB/Simulink/SimPowerSystems for electrolyser start-up phase and steady state operation are also presented.
An illustration on the global schemes for modelling of the electrolyzer, as well as utilities (i.e. compressor) and hydrogen storage tank is done by Zhou and Francois [22] using Casual ordering graph (COG). COG is a proposition of symbolism for transcribing thought which helps to describe dynamic systems in a physical and unambiguous manner. The research article, [22] discusses the control oriented electrolyzer model which is again based on Ullebergs model [19]. However unlike Ulleberg's model, the thermal model in [22] is replaced by a constant external temperature which can be specified manually.
In most applications, the hydrogen from alkaline electrolysis is needed to be at higher pressures (like fuel cell electric vehicles). The power required for high pressure water electrolysis, wherein water is pumped to higher pressure may be less than the power required for atmospheric water electrolysis wherein the pressure of produced gaseous hydrogen is compressed, since the pump power for water is much less than that for hydrogen gas. In the study done in [17] , the ideal water electrolysis voltage up to 70 MPa and 250 C, is estimated by referring to both the results of LeRoy et al. [14] up to 10 MPa and 250 C, and the latest steam tables. The study concluded that using high- pressure water electrolysis, the power required to produce high pressure hydrogen by water electrolysis is estimated to be about 5% less than that required for atmospheric water electrolysis, assuming compressor and pump efficiencies of 50%. However, in our study this avenue is not explored as the mathematical description is based on Ulleberg's model.
Interestingly, the modelling and control of alkaline electrolyzer can also be done using data driven approach for system identification as discussed in [5]. The electrolysis process model was developed using a nonlinear identification technique based on Hammerstein structure. The electrochemical electrolysis was carried out in an electrolyzer composed of 12 series connected steel cells with a 30 wt.% solution of KOH. Model Predictive Control (MPC) is used to control the energy consumption of the developed electrolyzer.
The hydrogen production, storage and conversion subsystems are studied in detail in [21]. A comprehensive mathematical model for hydrogen storage is derived to get a closer insight into the total system efficiency and different loss mechanisms. This research is originally intended to study the seasonal storage of hydrogen from a small self-sufficient solar hydrogen pilot plant at Helsinki University of Technology. The concepts discussed in this

article can be extended to present work on the pressurized hydrogen storage.
A system of alkaline electrolyzers is investigated in [12]. Experimental measured data from a 150 kW alkaline water electrolyzer is used for the development of a simulator model. The prediction of the temperature and efficiency for the different scales of electrolyzers (1 MW and 5 MW) was done using the developed model to investigate performance with regard to large scale hydrogen production. The two larger electrolyzers were not actual systems and they were only considered for simulation purposes. The performance of the combination of large and small electrolyzers was predicted and compared.
The discussion on the product gas purity in alkaline water electrolysis is presented in [7]. This article describes mathematical model for an electrolyzer based purely on first principles and presents the electrolysis cell through coupled continuously stirred tank reactors. Mass transfer phenomena between the phases are explained through the application of Reynolds and Sherwood correlations.
A review on the status of water electrolysis for energy system is presented in [4]. This review provides necessary understanding of electrolysis fundamentals and technologies for techno-economic analysis of water electrolysis-based concepts. It compares the alkaline electrolysis (AEL), PEM electrolysis (PEMEL) and solid oxide electrolysis (SOEL) in terms of available capacity, nominal and part load performance, flexibility, lifetime and investment costs. It concludes that the AEL is the most mature technology and can be adapted most easily to the present requirements.

1.6 Structure of the report

The following chapter of this report (Chapter 2) introduces the reader to the development of mathematical model for the alkaline electrolyzer plant. Chapter 3 presents the open loop analysis of steady state and dynamic simulation of the developed plant model.The controllability studies can be found in the Chapter 4. Finally, conclusions and the recommendations for future work are given in Chapter 5.

Chapter 2

Model Development

In this section, the development of model is described. Detailed electrolyzer plant flowsheet is introduced first to give an overview of the hydrogen production plant using alkaline water electrolysis and after that two different scenarios for the plant operation are described.
The model developed in this work focuses on the four basic sub domains of the electrolyzer plant, i.e. electrolyzers assembly, lye circulation system, compressor and the gas storage. The model has flexibility of selecting number of electrolyzers and here in this study it is assumed to consist of 3 electrolyzers that have different performance characteristics. In order to capture practical scenario, all the electrolyzers share a common rectifier i.e. the voltage across each electrolyzers is same. The dynamic model simulation is initialized using the steady state solution. It is assumed that the temperature of the circulating lye solution at steady state operation is 65 °C. However,it should be noted that the initial lye temperature at steady state can also be estimated by formulating an optimization problem that takes into account all the electrolyzers parameters and provides the best nominal lye temperature for the maximum economic profit. This is not the focus of present study and can be explored in future studies.
CasADi framework is used for the symbolic modeling in MATLAB. The system of Differential-Algebraic Equations (DAE) is solved using numerical integrator IDAS, available in the open-source software SUNDIALS suite. The MATLAB code is included in Appendix.

2.1 Plant Flowsheet and Problem Definition

The simplified flowsheet of the alkaline water electrolyzer plant investigated in this work is shown in figure 2.1. The electrolyzer plant consists of following basic sections:

- Electric power supply: Water electrolysis requires direct current supply therefore, it is necessary to convert the normal alternating current from power source to direct electric supply. This is done using rectifier and in practical scenario, multiple electrolyzers share a common transformer to lower the supply voltage to operating

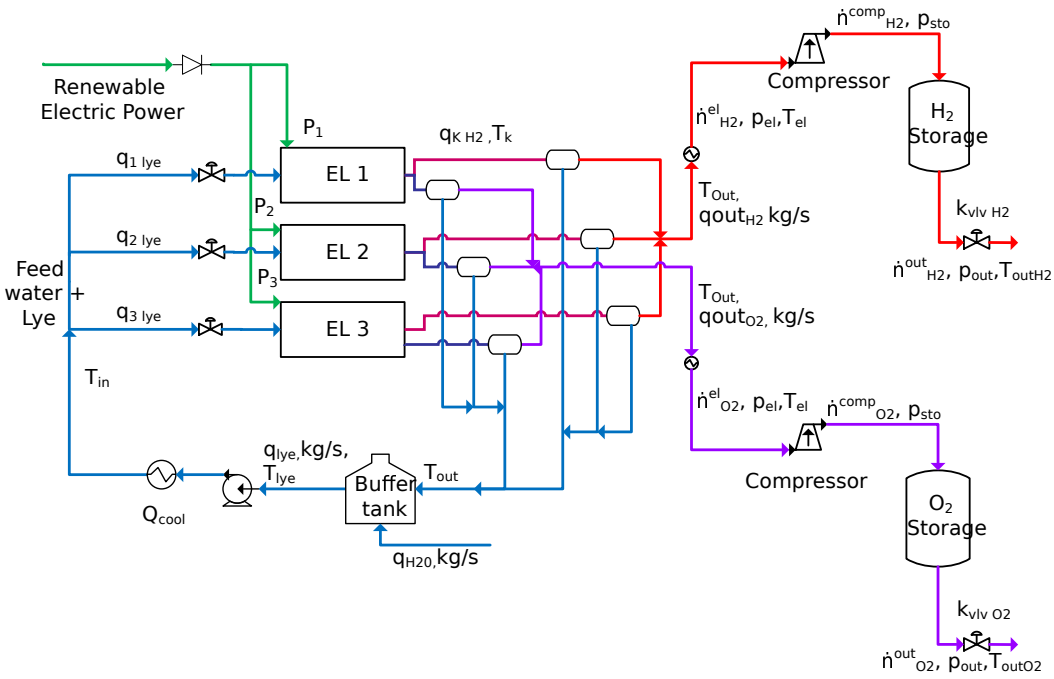

Figure 2.1: Flowsheet of alkaline water electrolyzer plant

voltage before rectifier converts the supplied alternating current to direct electric current. This means, all the electrolyzers with shared transformer operate across a common voltage.

- Electrolyzers: Water is splitted to hydrogen and oxygen using DC power supply and lye feed as inputs. All the electrolyzers are assumed to have same number of cells but different performance characteristics is obtained because of different parameter values. In this study because electrolyzers share a common transformer therefore overall hydrogen produced by the assembly of electrolyzers is dictated by the best performing electrolyzer.

- Gas separators and lye circulation system: The produced gas-liquid mixture from anodic (O_2 and lye) and cathodic (H_2 and lye) chambers of the electrolyzers is separated in gas separators. The liquid lye recovered from gas separators is mixed with additional water in the buffer tank to maintain electrolyte concentration and then chilled using heat exchangers before it is recycled back as feed to the electrolyzers.

- Gas purification and storage: The hydrogen and oxygen obtained from the gas separators is dried to remove residual traces of electrolyte and compressed using pump after which it is sent to pressurised vessels for storage.

This study also explores two different control strategies to counteract the disturbances in the input power. Degree of freedoms available in both the scenarios can be described using

the flowsheet in figure 2.1.

2.1.1 Case 1: Only electrolyzer voltage is available as manipulated variable to counteract disturbances in input power

This scenario corresponds to the most basic operation strategy wherein the voltage across each electrolyzer is same and is used as a manipulated variable for achieving flexibility in the performance of the electrolyzers. The temperature is not controlled and therefore is expected to vary significantly based on the disturbances in the input power.
The degree of freedom available for this electrolyzer plant are:

- Voltage, V across electrolyzer. The electrolyzers in this study study share a common rectifier, therefore voltage is same for all the electrolyzers.
- Duty Q_{cool} of the cooler in the recirculation loop.
- Valve opening of the outlet flow valves for the hydrogen and oxygen storage tanks, z_{H2} and z_{O2}.

2.1.2 Case 2: Both electrolyzer voltage and inlet lye flow rates are available as manipulated variables to counteract disturbances in input power

This scenario corresponds to the operation strategy wherein electrolyzer voltage, V and inlet lye flow rates q_{1lye}, q_{2lye} and q_{3lye} are used as manipulated variables. Availability of inlet lye flow rates makes it possible to maintain the temperature of electrolyzers and therefore, performance of the electrolyzers is better when compared to the Case 1.
The degree of freedom available for this electrolyzer plant are:

- Voltage, V across electrolyzer. The electrolyzers in this study study share a common rectifier, therefore voltage is same for all the electrolyzers.
- Splitted inlet lye flow rates q_{1lye}, q_{2lye} and q_{3lye} to the electrolyzers
- Duty Q_{cool} of the cooler in the lye circulation loop.
- Valve opening of the outlet flow valves for the hydrogen and oxygen storage tanks, z_{H2} and z_{O2}.

It should be noted that these cases studies are not included included as a part of this project report, as the discussions in this report ends with the design of the regulatory control layer. The two case studies defined above constitute the problem statement for the design of supervisory layer control structure. These are included just to provide the reader a flavour of the example control problem that can be defined for the given system of electrolyzers.
In order to maintain flexibility of the developed model, the 4 sub domains i.e. electrolyzer, compressor, lye circulation system and gas storage are modelled independently. Following sections will describe the model equations and assumptions considered for modeling each of these domains.

2.2 Electrolyzer Modelling

The electrolyzer is modelled as a separate process unit involving interconnected thermodynamic, electrochemical and thermal effects. These effects are described using mathematical model described by Ulleberg [19].

2.2.1 Thermodynamic model

Thermodynamics provides a framework for describing reaction equilibrium and thermal effects in electrochemical reactors. It also provides basis for defining the driving forces for transport phenomena in electrolytes and led to the description of the properties of electrolyte solutions. In Ullebergs model, maximum electrolyzer temperature of 100 °C is assumed. In alkaline electrolysis the total reaction for water splitting is:

$$\mathrm{H_2O\ (l)} + \mathrm{electrical\,energy} \longrightarrow \mathrm{H_2\ (g)} + \frac{1}{2}\,\mathrm{O_2} \tag{2.1}$$

Following assumptions can be made about above reaction,[19]:

- Hydrogen and oxygen are ideal gases
- Water is an incompressible fluid
- The gas and liquid phases are separate

Based on these assumptions the total change in enthalpy ΔH, for splitting water is the enthalpy difference between the products and reactants. This is also true for the change in entropy ΔS.
The change in Gibbs energy ΔG, is expressed by

$$\Delta G = \Delta H - \mathrm{T}\Delta S \tag{2.2}$$

At standard conditions (25°C and 1 bar) the change is Gibbs energy is positive as the splitting of water is non-spontaneous. The standard Gibbs energy for water splitting is ΔG°= 237 kJ/mol. For an electrochemical process operating at constant pressure and temperature the maximum possible useful work (i.e. the reversible work) is equal to the change in Gibbs energy ΔG. Faradays law relates the electrical energy (emf) needed to split water to the chemical conversion rate in molar quantities. The emf for a reversible electrochemical process, or the reversible cell voltage, is expressed by

$$U_{rev} = \frac{\Delta G}{\mathrm{zF}} \tag{2.3}$$

The total amount of energy needed in water electrolysis is equivalent to the change in enthalpy ΔH. The change in Gibbs energy ΔG, includes thermal irreversibilities TΔS, which is equal to heat demand for a reversible process. The standard enthalpy for water splitting is, ΔH°= 286 kJ/mol.
The cell voltage at which the supplied energy participates both in ΔG and TΔS, and there is no heat generation or heat absorption from outside of the system is referred to as

thermoneutral cell voltage.
The total energy demand ΔH is related to the thermoneutral cell voltage by the expression

$$U_{tn} = \frac{\Delta H}{\mathrm{zF}} \tag{2.4}$$

At standard conditions U_{rev} = 1.229 V and U_{tn} = 1.482, but these will change with temperature and pressure. In the applicable temperature range, U_{rev} decreases slightly with increasing temperature, while U_{tn} remains almost constant. Increasing pressure increases U_{rev} slightly, while U_{tn} remains constant.

2.2.2 Electrochemical model

When direct current is supplied to the electrolysis cell to produce hydrogen, the cell voltage is always higher than reversible cell voltage (U_{rev}) because of irreversibilities. These irreversibilities are mainly overvoltages and parasitic currents that leads to energy losses in the cell and limit the cell efficiency. The overvoltage is composed of ohmic, activation and concentration voltages, i.e.

$$\mathrm{U} = U_{rev} + U_{ohm} + U_{act} + U_{con} \tag{2.5}$$

U_{ohm} is the overvoltage caused because of ohmic losses in the cell elements (electrodes, current collectors, interconnections, etc.). This U_{ohm} is proportional to the electric current that flows through the cell and imparts linear nature of the U-I characteristics curve as shown in the figure 2.2.
U_{act} is the activation overvoltage and is due to electrode kinetics.The charge transfer between the chemical species and the electrodes needs energy. This energy barrier that the charge has to overcome to go from the reactants to the electrodes and vice versa highly depends on the catalytic properties of the electrode materials. It causes an overvoltage across the electrodes, U_{act} . The anodic half-reaction produces a much higher activation overvoltage than the cathodic half- reaction. U_{act} is highly nonlinear and behaves with a logarithmic tendency with respect to the electric current flowing through the cell [20].
U_{con} is known as concentration voltage, this is caused because of mass transport processes (convection and diffusion). Transport limitations reduce reactant concentration while creating higher concentration of products at the interface between the electrode and the electrolyte. However, in case of alkaline electrolysis this U_{con} is significantly smaller than U_{ohm} and U_{act} and is therefore, not considered in this study.
The electrode kinetics is modeled using empirical voltage-current (U-I) relationships as given in [19]

$$\mathrm{U} = U_{rev} + \frac{r_1 + r_2\mathrm{T}}{\mathrm{A}}\,\mathrm{I} + \mathrm{s}log_{10}\left(\frac{t_1 + \frac{t_2}{\mathrm{T}} + \frac{t_3}{T^2}}{\mathrm{A}}\,\mathrm{I} + 1\right) \tag{2.6}$$

Here, r_1 and r_2 are ohmic resistance parameters, s, t_1, t_2 and t_3 are overvoltage coefficients and A is the electrode area.
The performance of a electrolyzer is characterized by plotting the cell voltage against the current density as shown in figure 2.2.
The electrochemical performance is highly dependent on the process temperature. Figure

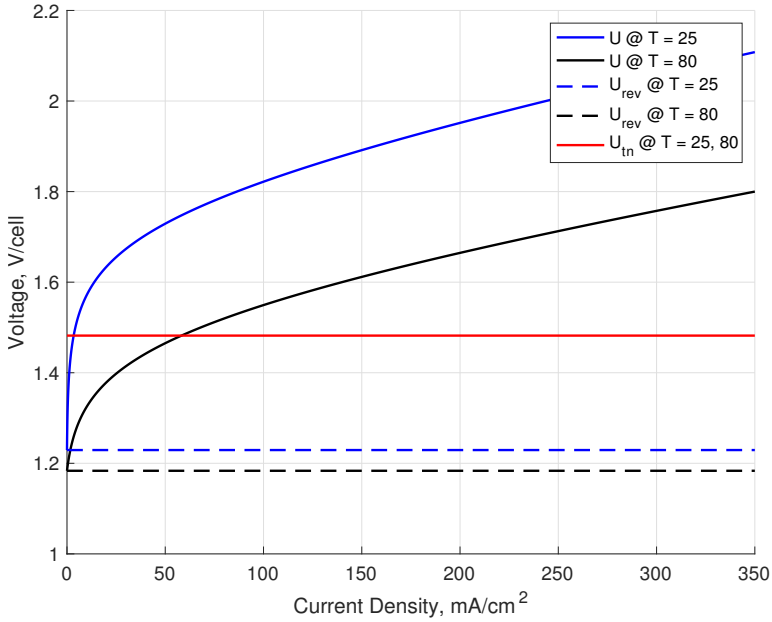

Figure 2.2: U-I curve for a typical electrolyzer

2.2 shows U-I characteristic curves of an alkaline electrolyzer for operation temperature of 25 °C and 80 °C. These U-I curves typically use current density to make it possible to compare cells with different electrode surface areas. As clearly shown in the figure 2.2 increase in temperature for a given current reduces reversible cell voltage, ohmic and activation overvoltages which also reduces the cell voltage. However, increasing current at a given temperature increases cell voltage and the related overvoltages.
At lower current densities, logarithmic relationship is observed which suggests that activation phenomena is predominant while at the higher current density ohmic losses are considerable. The cell voltage and consequently cell power consumption is lower at higher temperatures for any current density.
The U-I curves in figure 2.2 shows that when cell voltage is lower than U_{rev}, the cell current is zero and electrolysis reaction cannot take place. At lower current densities when cell voltage lies between U_{rev} and U_{tn}, external heating is needed for electrolysis to happen. However, when the cell voltage is higher than U_{tn}, the supplied power is always greater than the minimum power required for electrolysis process to occur and electrolysis process will occur spontaneously. The water electrolysis at these values of cell voltage is exothermic and generates heat which is proportional to (U_k - U_{tn}) where U_k is the operating cell voltage.
Faraday efficiency is defined as the ratio between the actual and theoretical maximum amount of hydrogen produced in an electrolyzer. Faraday efficiency is caused by the parasitic current losses and the contamination of electrolyte because of dissolution of H_2 in O_2. The fraction of parasitic currents to total current increases with decreasing current densities. Also, an increase in temperature will reduce resistance that increases parasitic current

and lowers Faraday efficiency. An empirical relation given by [19] accurately depicts this phenomena for a given temperature as:

$$\eta_F = \frac{(\frac{\mathrm{I}}{\mathrm{A}})^2}{f_1 + (\frac{\mathrm{I}}{\mathrm{A}})^2} f_2 \tag{2.7}$$

Here, f_1 and f_2 are parameters related to Faraday efficiency. According, to Faradays law hydrogen production rate in an electrolyzer cell is proportional to transfer rate of electrons at the electrodes, which in turn is equivalent to the electrical current in the external circuit. Hence, hydrogen production rate in an electrolyzer which consists of several cells connected in series, is given as

$$\dot{n}_{H_2} = \eta_F \frac{n_C \mathrm{I}}{\mathrm{zF}} \tag{2.8}$$

The water consumed during the electrolysis process and be calculated from stoichiometry eq. (2.1) i.e.

$$\dot{n}_{H_2O} = \dot{n}_{H_2} = 2\,\dot{n}_{O_2} \tag{2.9}$$

Another important parameter for electrolyzer is electrical efficiency η_e. Electrical efficiency is defined as the ratio of thermoneutral voltage (U_{tn}) to the cell voltage (U),

$$\eta_e = \frac{U_{tn}}{\mathrm{U}} \tag{2.10}$$

It represents the ratio between energy contained in the hydrogen produced to the energy needed to electrolyze the water consumed during the process. For a given temperature, increasing current density increases cell voltage that in turn reduces electrical efficiency. However, at given current density, increasing temperature reduces cell voltage which increases electrical efficiency.

2.2.3 Thermal model

Thermal balance for the electrolyzer can be written on per stack basis using lumped thermal capacitance model. The schematic of an electrolyzer is shown in the figure 2.3

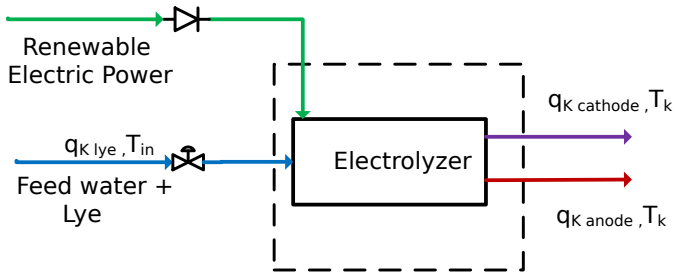

Figure 2.3: Schematic of the electrolyzer

$$\dot{Q}_{acc} = \dot{Q}_{in} - \dot{Q}_{out} + \dot{Q}_{gen} - \dot{Q}_{loss} \tag{2.11}$$

$\dot{Q}_{acc}$ is the energy accumulated in the electrolyzer, $\dot{Q}_{in}$ is thermal energy of the incoming lye feed, $\dot{Q}_{out}$ is the thermal energy of outlet streams leaving anodic and cathodic sections of the electrolyzer. $\dot{Q}_{gen}$ is the second term on the right- hand side of eq. (2.12) and is the internal heat generated in the electrolyzer when it is operated at voltages above thermoneutral voltage. $\dot{Q}_{loss}$ is the total heat loss to the ambient and is calculated using convective cooling relationship as given by the third term on the right hand side of eq. (2.12). The dynamic energy balance of the k^{th} electrolyzer is represented as

$$C_t \frac{\mathrm{d}T_k}{\mathrm{dt}} = q_{klye}\, C_{plye}(T_{in} - T_k) + n_{ck}\,(U_k - U_{tn})I_k - \frac{1}{R_t}(T_k - T_a) \tag{2.12}$$

where t is in seconds, C_t and R_t are overall thermal capacity and thermal resistance of the electrolyzer and are constants that need to be known prior to solving the thermal equations. It is assumed that there is no mass accumulation in the electrolyzer during operation and heat capacity C_{plye} of inlet and outlet streams is same.

2.3 Lye Circulation System

The gas-lye mixture generated from electrolyzers is separated in the gas separators. For simplicity, the gas separators are assumed to be ideal and losses in the separation process are neglected. The enthalpy of gas streams produced (H_2 and O_2) is assumed to be equal to the enthalpy of water consumed during electrolysis process.
Electrolyte is collected in the buffer tank and additional water is added to maintain lye at a constant concentration in the electrolyzer system. In order to keep the developed model simple, temperature of additional water added to the lye is assumed to be equal to the temperature of liquid in the buffer tank. Heat capacity of 30% KOH electrolyte is assumed to be 3.1 J/g°C.
Figure 2.4 shows the control volumes considered for modeling of the lye circulation system. The temperature of the lye after mixing electrolyte streams from all the electrolyzers is given by

$$T_{out} = \frac{\Sigma(q_{klye} \cdot T_k \cdot C_{plye}) - \Sigma(q_{kH2Oloss} \cdot T_k \cdot C_{pw}) + \Sigma(q_{kH2Oloss}) \cdot (C_{pw} - C_{lye}) \cdot T_{ref}}{\Sigma q_{klye} \cdot C_{plye} - \Sigma q_{kH2Oloss} \cdot C_{plye}} \tag{2.13}$$

where $q_{kH2Oloss}$ is the flow rate of the water consumed during electrolysis and is calculated using eq. (2.9). T_k and q_{klye} are the temperature and inlet lye flow rate of the k^{th} electrolyzer. C_{pw} and C_{plye} are the heat capacities of water and the lye solution respectively.
During nominal operating conditions, before recirculating lye solution it is cooled by the heat exchanger to the desired inlet temperature, T_{in} which is set to 65 °C for this study. The energy balance for the heat exchanger is given as,

$$Q_{cool} = q_{lye} \cdot C_{plye} \cdot (T_{out} - T_{in}) \tag{2.14}$$

At the split point, the lye is divided to three electrolyzers and,

$$q_{lye} = q_{1lye} + q_{2lye} + q_{3lye} \tag{2.15}$$

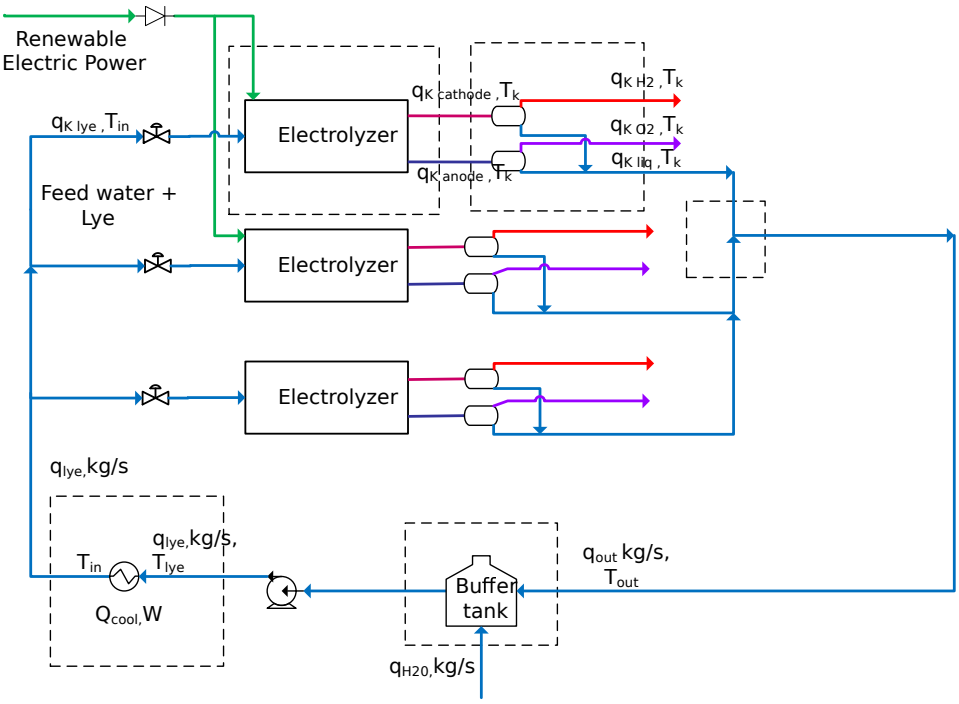

Figure 2.4: Schematic of the lye circulation system. The control volumes are marked with a dashed line

Here, it is to be noted that changing inlet lye flowrate to any electrolyzer q_{klye} will change the net lye flowrate, q_{lye} through the electrolyzer assembly.

2.4 Compressor

The hydrogen from the atmospheric electrolyzer is at atmospheric pressure and therefore, a compressor is needed to compress hydrogen to high pressure storage tank, as shown in figure 2.1. The compressors available in process industry today can be categorized in two distinct categories: reciprocating and rotary compressors.
For this study, variable speed centrifugal compressor is selected. For simplicity, it is assumed that all the power required by the compressor to perform operation is available, that is there is perfect control of the compressor power.
Centrifugal compressor is a type of rotary compressor that compress gas using centrifugal force. In a centrifugal compressor, impeller and the shaft are only moving parts and it consists of a housing with flow passages for gas. Work is done on the gas by the impeller mounted on rotating shaft. Gas is then discharged at a high velocity into a diffuser where the velocity is reduced and its kinetic energy is converted to static pressure.
The calculation of the performance of centrifugal compressors is based on a polytropic

compression step. The polytropic process is expressed as

$$PV^x = \text{constant} \tag{2.16}$$

where, x denotes the polytropic exponent and P, V represents pressure and volume of the process. This polytropic compression describes the actual process involving both heat transfer and friction happening within the compressor. The relationship between molar flowrate of hydrogen out of the compressor, $\dot{n}_{H2}^{comp}$ and compressor power is [22]

$$\dot{n}_{H2}^{comp} = \frac{\alpha}{\mathrm{w}} Power_{comp} \tag{2.17}$$

and

$$\mathrm{w} = \frac{\mathrm{xR}T_{el}}{\text{x-1}} \left[\frac{p_{sto}}{p_{el}}^{\frac{\mathrm{x}-1}{\mathrm{x}}} \right] \tag{2.18}$$

where w is the polytropic work, α is the compressor efficiency, and $Power_{comp}$ is compressor power, T_{el} and p_{el} are inlet gas temperature and pressure to the compressor, p_{sto} is the outlet gas pressure from the compressor and is equal to the hydrogen pressure in the storage tank and R is the gas constant.
As shown in the plant flowsheet, (figure 2.1) $\dot{n}_{H2}^{comp}$ is assumed to be equal to the total flowrate of hydrogen out from all the electrolyzers, $\dot{n}_{H2}^{el}$.
Solving eq. (2.17) and (2.18) for $Power_{comp}$,

$$Power_{comp} = \frac{\dot{n}_{H2}^{comp}}{\alpha} \cdot \frac{\mathrm{xR}T_{el}}{\text{x-1}} \left[\frac{p_{sto}}{p_{el}}^{\frac{\mathrm{x}-1}{\mathrm{x}}} \right] \tag{2.19}$$

A centrifugal compressor is a type of rotary compressor and has fixed pressure ratio, therefore $Power_{comp}$ is a dependent variable that is calculated from eq. (2.19)
As given in [3] the polytropic exponent, x is related to adiabatic component γ, through polytropic efficiency E_p as,

$$\frac{x-1}{\mathrm{x}} = \frac{\gamma-1}{\gamma} \cdot \frac{1}{E_p} \tag{2.20}$$

The polytropic efficiency of the centrifugal compressor is between 0.7 to 0.75 as mentioned in [3]. For the calculations in this study, it is assumed that E_p = 0.75. The adiabatic exponent γ for hydrogen which is a diatomic molecule is 1.4. For this study, from eq. (2.20) polytropic exponent x = 1.62, which is used for all the simulations.

2.5 Gas Storage

2.5.1 Hydrogen Storage

The overall mole balance of a gas storage, as shown in figure 2.5 can be expressed as

$$\frac{\mathrm{d}n_{sto}}{\mathrm{dt}} = \dot{n}_{H2}^{comp} - \dot{n}_{H2}^{out} \tag{2.21}$$

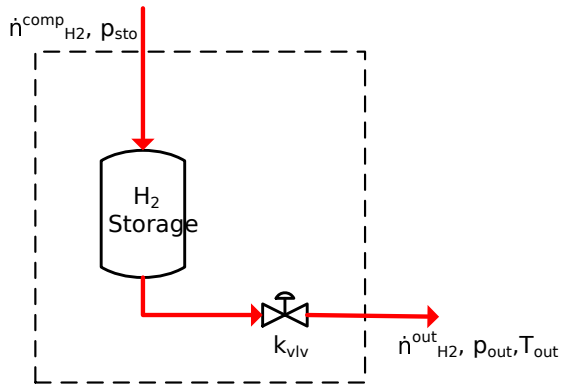

Figure 2.5: Schematic diagram of H_2 gas storage. The control volume is marked with a dashed line

where n_{sto} is the molar holdup in the storage tank and $\dot{n}_{H2}^{out}$ is the molar outlet flow. Inserting ideal gas $n = PV/RT$ in eq. (2.21)

$$\frac{\mathrm{d}p_{sto}}{\mathrm{dt}} = \frac{(T_{sto} + 273.15)\mathrm{R}}{V_{sto}}(\dot{n}_{H2}^{comp} - \dot{n}_{H2}^{out}) \tag{2.22}$$

where V_{sto} is the storage volume, T_{sto} is the storage temperature in °C and R is the gas constant. The operating pressure storage p_{sto} is the dynamic state variable.
The outlet molar flow is given by the valve equation

$$\dot{n}_{H2}^{out} = k_{vlv}\, z\, \sqrt{\mathrm{p_{sto}} - \mathrm{p_{out}}} \tag{2.23}$$

Here k_{vlv} is the valve constant and z is the valve displacement. The storage temperature T_{sto} is assumed to be ideally controlled to 25 °C. The pressure of the electrolyzer is assumed to be constant. The pressure in the vessel increases as it is filled with more gas. However, the pressure of the inlet stream does not change. Note that the pressure of the inlet stream must be higher than the storage pressure in order to get it into the storage.

2.5.2 Oxygen Storage

The oxygen production is calculated directly from the stoichiometry of the electrolysis reaction as given by eq. (2.9).
The overall mole balance for oxygen gas storage is given by eq. (2.21), and assuming ideal gas behaviour the equation becomes

$$\frac{\mathrm{d}p_{sto}}{\mathrm{dt}} = \frac{(T_{sto} + 273.15)\mathrm{R}}{V_{sto}}(\dot{n}_{O_2}^{comp} - \dot{n}_{O_2}^{out}) \tag{2.24}$$

There is no accumulation of gases in the compressor, therefore $\dot{n}_{O_2}^{comp} = \dot{n}_{O_2}^{el}$. Similar to the hydrogen storage, T_{sto} is ideally controlled at 25 °C.
The outlet molar flow is given by the valve equation

$$\dot{n}_{O_2}^{out} = k_{vlv}\, z\, \sqrt{\mathrm{p_{sto}} - \mathrm{p_{out}}} \tag{2.25}$$

Chapter 3

Open Loop Analysis

In this chapter a study on the open loop behaviour of the electrolyzer plant is discussed. In the first section, a steady state analysis of the electrolyzer is performed. This study helps to identify parameter values for three differently performing electrolyzers. Once the parameter values for the electrolyzers are finalized, the effect of temperature on the performance characteristics of the three electrolyzers is shown.
Thereafter in the second section, the inlet lye flowrate and the volume of hydrogen and oxygen storage tanks are calculated.
Finally, in the last section of this chapter the dynamic behaviour of the entire plant is analyzed.

3.1 Steady-state analysis of the electrolyzers

The value of all parameters in the empirical U-I relationship (see eq. (2.6)) used to model electrode kinetics of the electrolyzer is given in the article by Ulleberg [19]. In practice, the performance of individual electrolyzers can be different based on their operational lifetime. Specific electricity consumption can be used to characterize the performance of the electrolyzers. It is defined as the ratio of electricity consumed in MWh per tonne of hydrogen (H_2) produced. This value is between 44 to 55. Lower values around 44 represent a newly installed electrolyzer with best performance and higher values closer to 55 represent that the electrolyzer is degraded and should be replaced. Therefore, the parameters for different electrolyzers as given in Appendix A are selected such that they represent electrolyzers at different stage of their operational lifetime.
The lower cell voltage corresponds to reduced power consumption and thus lower operation costs. On the other hand, electrolyzer design at higher current densities is expected to reduce capital investment costs in future [13]. However, higher current densities also corresponds to increased ohmic resistances and elevated overpotentials at anode and cathode. Therefore in this study, the current density of 350 mA/cm^2 is taken as the highest allowable value for the operation of electrolyzer system when 63kW of power is supplied. At nominal operation condition, lye is entering to electrolyzer assembly at 65 °C and the

hydrogen production rate is 14.44 Nm^3/hr.

3.1.1 Effect of temperature on the electrolyzers

In this section the effect of temperature on the electrolyzer performance is discussed. For a given current density, higher temperature leads to reduced cell voltage (see figure 3.1). Also, from figure 3.1 we see that for both the temperature values, at a given current density, electrolyzer 2 has the lowest cell voltage and thus lower operational cost. Therefore, electrolyzer 2 is the best performing electrolyzer. In practice, when constant voltage is

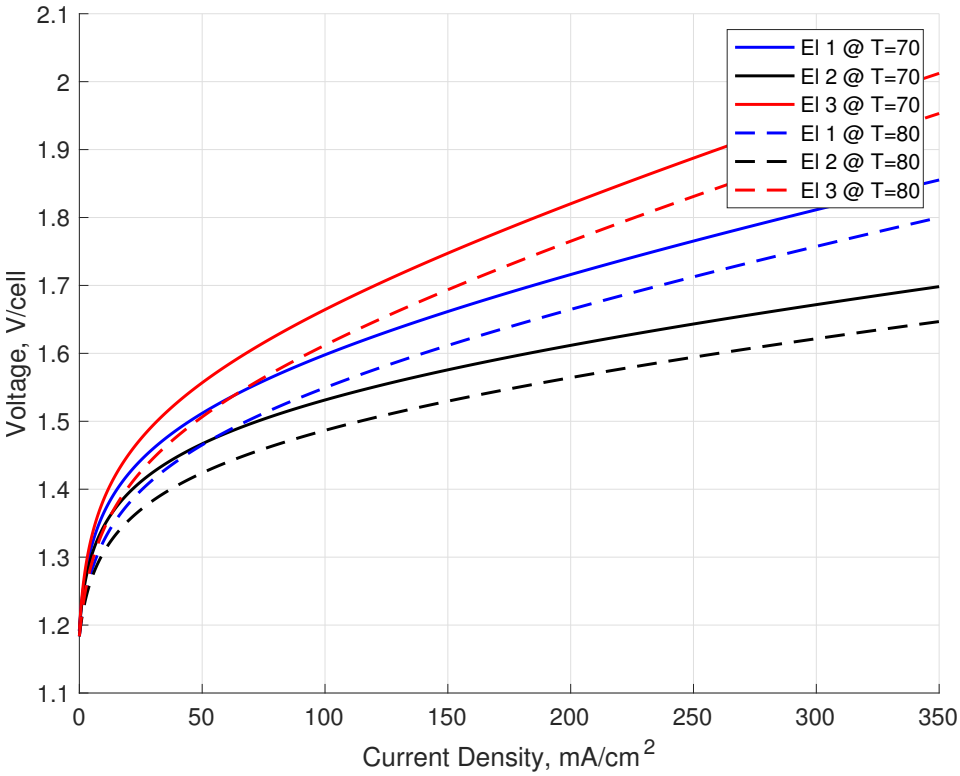

Figure 3.1: Effect of temperature on electrolyzer performance

maintained across all the electrolyzers, the best performing electrolyzer dictates current distribution in all the electrolyzers. It is also evident from figure 3.1 that the increase in temperature at a given cell voltage increases the current density quite significantly. As discussed earlier, current densities higher than 350 mA/cm^2 are not preferable for the electrolyzer operation and therefore the temperature of the electrolyzer system should be carefully controlled to achieve consistent performance. Figure 3.2 shows the specific electricity consumption of three electrolyzers at different temperatures (70 °C and 80 °C). As expected at higher temperature for a given current density, cell voltage is reduced which translates into lower specific electricity consumption and therefore lower operating costs.

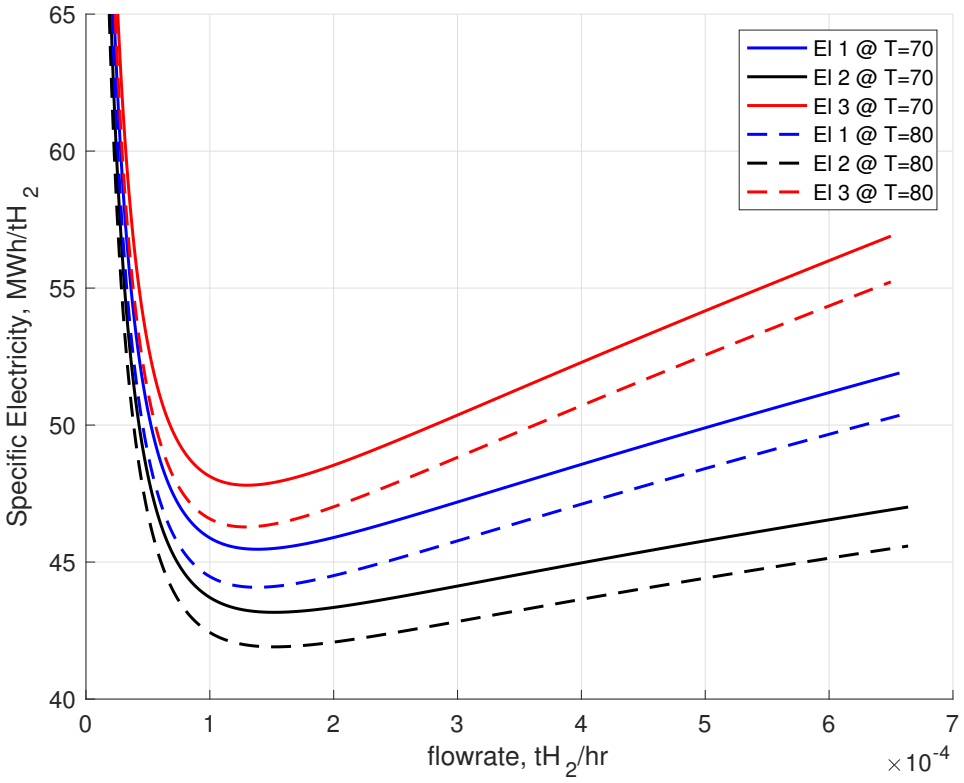

Figure 3.2: Effect of temperature on specific electricity consumption

However at low loads, energy consumption increases dramatically (see figure 3.2). This is poor performances of electrolyzers can be due to gas permeation through the membrane, parasitic reactions and leakage current at the stack level [2]. At low current densities, these phenomena can become predominant over water decomposition reaction itself and consequently, there is increase in the specific electricity consumption.
Higher operating temperature at a given cell voltage has higher current density which is helpful to reduce the investment costs associated to alkaline electrolysis [13] but is disadvantageous because of high corrosive effects of the electrolyte at high temperature values [11]. This manifests itself as an interesting design problem and therefore sufficient attention should be given in selection of the nominal operating conditions for the electrolyzer system.

3.2 Calculation of inlet lye flowrate and the volume of storage tanks

Lye flowrate is an important design parameter because it decides the size of the electrolyzer assembly. Therefore, it needs to be set such that there is sufficient lye for the operation of

electrolyzer assembly. As discussed in previous chapter, inlet lye temperature is 65°C and a temperature rise of 15 °C is assumed to be present across each electrolyzer at nominal operating conditions. Solving numerically, the lye flowrate is found to be 83 g/s for each electrolyzer.
The volume of gas storage tanks is dependent on the maximum design pressure, production rate and the production volume that we desire to store. In this study, the storage tanks are designed to a maximum pressure of 30 bar and have capacity to hold 6 hr of production volume. Minimum storage pressure of the gas (both H_2 and O_2) in the storage tank is 20 bar for the outlet supply pressure is 19 bar, with a constant pressure drop of 1 bar across the outlet value. With given specifications and assuming that gases behave ideally, volume of storage tank is given as

$$\mathrm{V} = \frac{n_{H2}\mathrm{RT}}{\Delta \mathrm{P}} \tag{3.1}$$

where, n_{H_2} is the moles of hydrogen produced in 6 hours during nominal operation conditions and ΔP is the maximum pressure differential across the outlet value i.e. 10 bar. Using above eq. (3.1) volume of hydrogen tank is calculated to 9500 litres.
From stoichiometry volume needed for oxygen storage is half of the volume required for hydrogen storage at same storage conditions. Hence, the volume of oxygen storage tank is 4750 litres.

3.3 Dynamic Analysis of the electrolyzer system

To integrate alkaline electrolysis in the production of hydrogen for industrial processes, it is necessary that the electrolyzer assembly should be sufficiently flexible to allow operation in variable power scenarios. Hence, the dynamic behaviour of the alkaline water electrolyzer plant has to be analysed. This is done by performing an open loop dynamic analysis of the system.
Before we start designing the control system it is important to decide which process variables should be controlled using the available degree of freedoms (MVs). That is why, step response analysis is carried out to understand the response of candidate control variables which are electrolyzer current, cell voltage, electrolyzer power, electrolyzer temperature, outlet lye temperature and hydrogen production rate.

3.3.1 Effect of step in the inlet lye flow rate on Open-loop system

Step change in the inlet lye flowrate to the electrolyzer 1, q_{1lye}

As shown in figure 3.3, q_{1lye} is increased by +20% at t = 3000s and the response of dependent variables to this change is analyzed for 12 hours.

The increase in the lye flowrate to electrolyzer 1 will increase the temperature of lye at the inlet of electrolyzer T_{in} (see figure 3.4) since more feed coming in for the exothermic water splitting reaction to happen when the cooling duty of the heat exchanger in the lye circulation loop Q_{cool} is held constant.
For electrolyzer 2 and 3, the increase in T_{in} for the lye (at constant lye flowrate) means

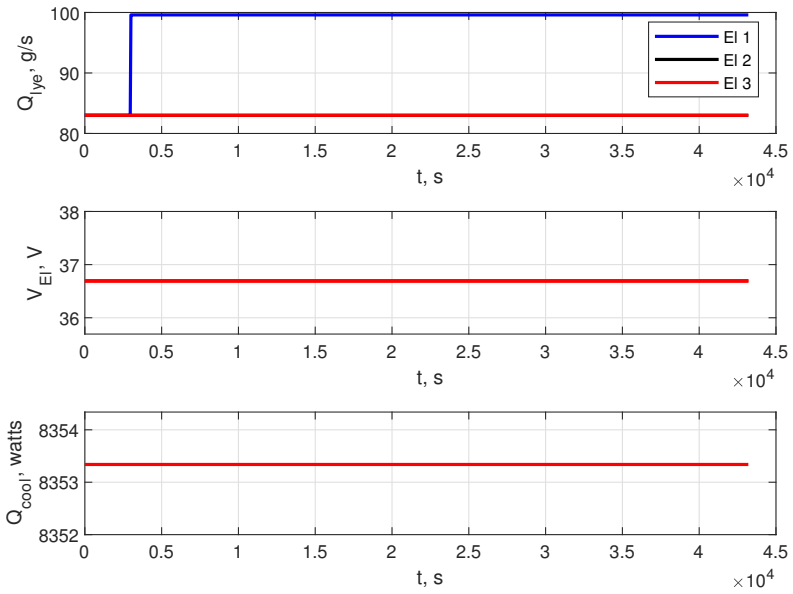

Figure 3.3: +20% step in the inlet lye flowrate to Electrolyzer 1, while cooling duty Q_{cool} and electrolyzer voltage V are kept constant

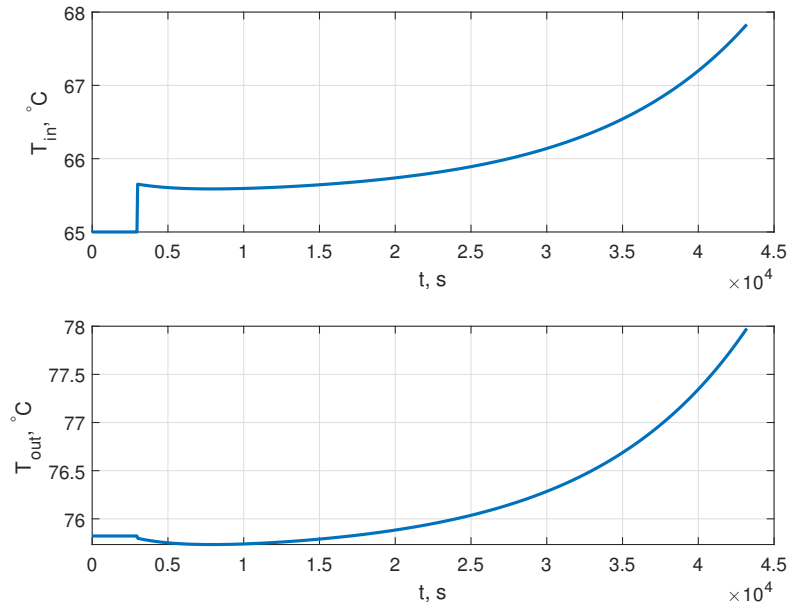

Figure 3.4: Response of inlet lye temperature T_{in} and outlet lye temperature from the electrolyzer assembly T_{out} to +20% step in inlet lye flowrate to Electrolyzer 1

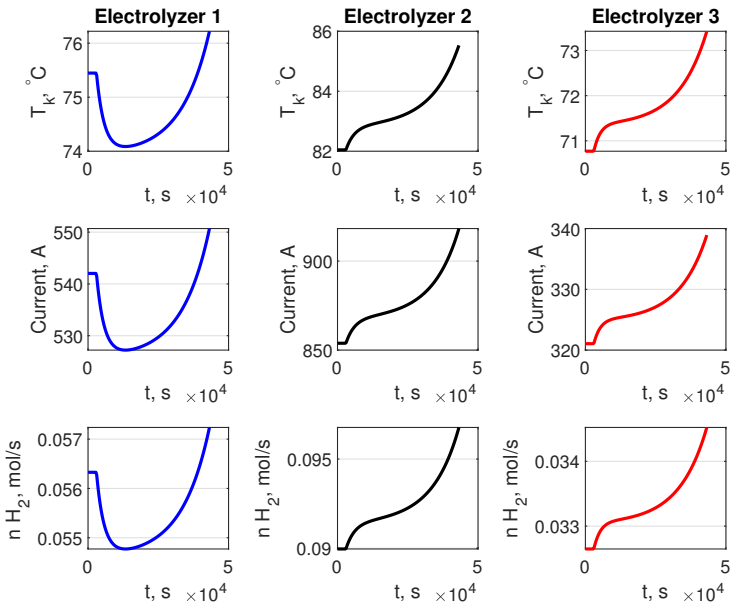

Figure 3.5: Responses to +20% step in inlet lye flowrate to Electrolyzer 1

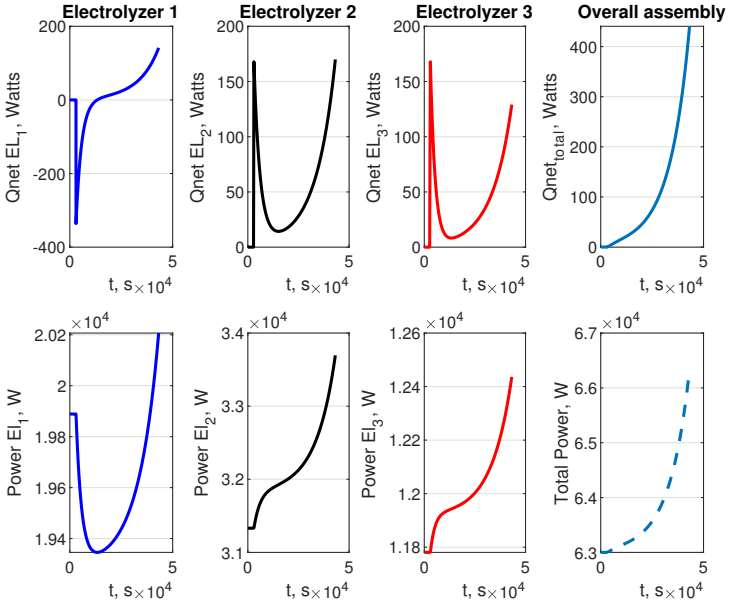

Figure 3.6: Response of total heat enthalpy and supplied power to +20% step in inlet lye flowrate to Electrolyzer 1

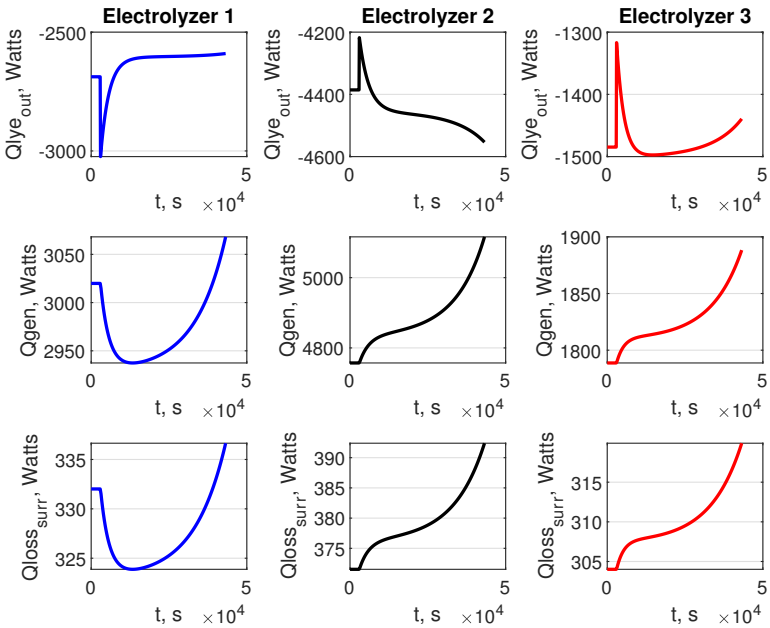

Figure 3.7: Responses of heat taken out by lye $Qlye_{out}$, heat generated inside electrolyzer $Qgen$ and heat loss in electrolyzer $Qloss_{surr}$ to +20% step in inlet lye flowrate to Electrolyzer 1

that more heat will be added and electrolyzer temperature starts to increase as seen in figure 3.5. For electrolyzer 1 the increase in inlet lye temperature should also increase the electrolyzer temperature. However, since the lye circulation for electrolyzer 1 is increased, more heat $Qlye_{out}$ is also removed (see figure 3.7) and the net effect is negative (see figure 3.6). Therefore the temperature of electrolyzer 1 is decreased (see figure 3.5). Also as seen from the figure 3.1, since temperature is directly linked to current density at constant cell voltage which in turn governs the hydrogen production from the electrolyzer therefore, other electrolyzer variables like electrolyzer current and hydrogen production from the electrolyzer have similar behaviour as the electrolyzer temperature (see figure 3.5).
Initially, T_{out} (i.e. temperature of mixed lye streams at the outlet before going into the buffer tank) decreases marginally (see figure 3.4).
Due to increase in temperature of electrolyzer 2 and 3 these will operate at higher current density (since given all electrolyzers are operating at constant voltage, figure 3.3), which will increase the power consumption and total heat generation, $Qnet_{total}$ (see figure 3.6). For electrolyzer 1, temperature is lowered initially and it will operate at less current. Since we have kept the amount of heat removed from the lye circulation (Q_{cool}) constant (see figure 3.3) the overall energy of the system increases and the temperature of lye out increases (see figure 3.4). This effect has a open loop positive feedback that increasing T_{out} makes system unstable.
This illustrates that with the assumptions used, the system is open loop unstable and needs to be controlled.

Step change in the inlet lye flowrate to the electrolyzer 2, q_{2lye}

As shown in figure 3.8 q_{2lye} is increased by +20% at t = 3000s and the response of dependent variables to this change is analyzed for 12 hours.
As discussed in section 3.1, electrolyzer 2 is the best performing electrolyzer and it dictates the performance of the overall electrolyzer assembly. This fact is validated in the figure 3.2, where we see that the electrolyzer 2 has least specific electricity consumption.
Similar to step in q_{1lye}, +20% step in q_{2lye} will also increase the temperature of lye at the inlet, T_{in} to all electrolyzers initially (see figure 3.9). For electrolyzer 1 and 3 increase in T_{in} (at constant lye flow rate) means that more heat will be added and the electrolyzer temperature starts to increase (see figure 3.10). This increase in T_{in} should also increase the temperature of electrolyzer 2. However, since the lye flow is also increased, more heat $Qlye_{out}$ is removed (see figure 3.11) and the net effect is negative $QnetEL_2$ as seen in figure 3.12 and the temperature of electrolyzer 2 decreases (see figure 3.10).
Also, as already established that there is a direct relationship between electrolyzer temperature, current and hydrogen production (at given cell voltage) therefore, in figure 3.10 we see similar responses between these electrolyzer variables. Initially, as seen in figure 3.9 there is marginal increase in T_{out} because of higher fraction of hot electrolyte stream coming out of electrolyzer 2.
Due to reduced temperature in electrolyzer 2 it will operate at lower current which will in turn reduce the power consumption (remember all electrolyzer are operating at constant voltage, see fig 3.8) and net heat $Qnet_{total}$ will be removed out of the electrolyzer assembly as depicted in figure 3.12. Since we keep the amount of heat removed in the lye circulation loop Q_{cool} constant (see figure 3.8) the overall energy in the system decreases and the T_{out} decreases. This effect has a open loop negative feedback that decreasing T_{out} makes the system unstable.
This again demonstrates that with the assumptions used the system is open loop unstable and needs to be controlled.

Step change in the inlet lye flowrate to the electrolyzer 3, q_{3lye}

As shown in figure 3.13 q_{3lye} is increased by +20% at t = 3000s and the response of dependent variables to this change is analyzed for t = 12 hours.
The response of electrolyzer 3 to step increase in the inlet lye flowrate is exactly similar to electrolyzer 1 and can be explained from the same cognition. Therefore, the observed behaviour of T_{in}, T_{out} and responses of individual electrolyzer variables are shown in the figure 3.23 and 3.15 respectively without providing any supporting explanations.

3.3.2 Effect of step in heat removed from lye circulation on open-loop system

As shown in figure 3.16 Q_{cool} is increased by +10% at t = 300s and the response of dependent variables to this change is analyzed for t = 3 hours. The inlet lye temperature, T_{in} and outlet lye temperature from the electrolyzer assembly T_{out} are both decreased (see figure 3.17) because there increase in the amount of the heat taken out by the cooling in the lye circulation loop for a given total lye flow through the electrolyzer assembly.

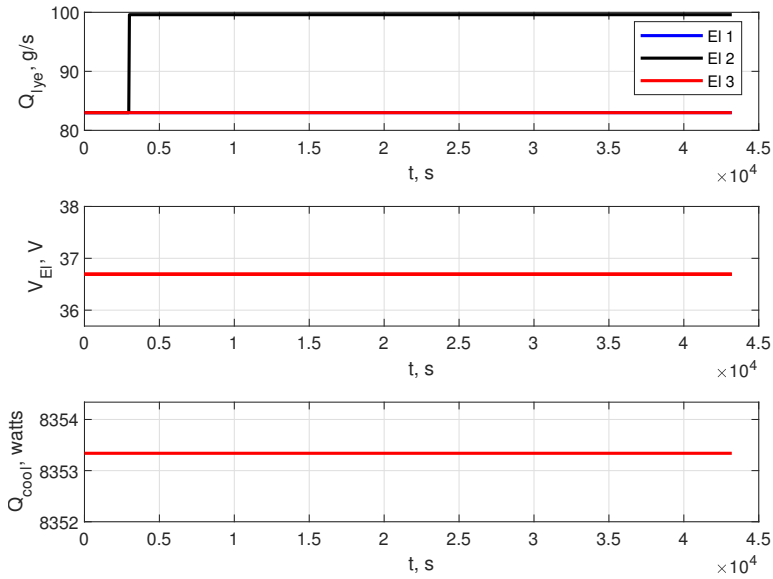

Figure 3.8: +20% step in the inlet lye flowrate to Electrolyzer 2, while cooling duty Q_{cool} and electrolyzer voltage V are kept constant

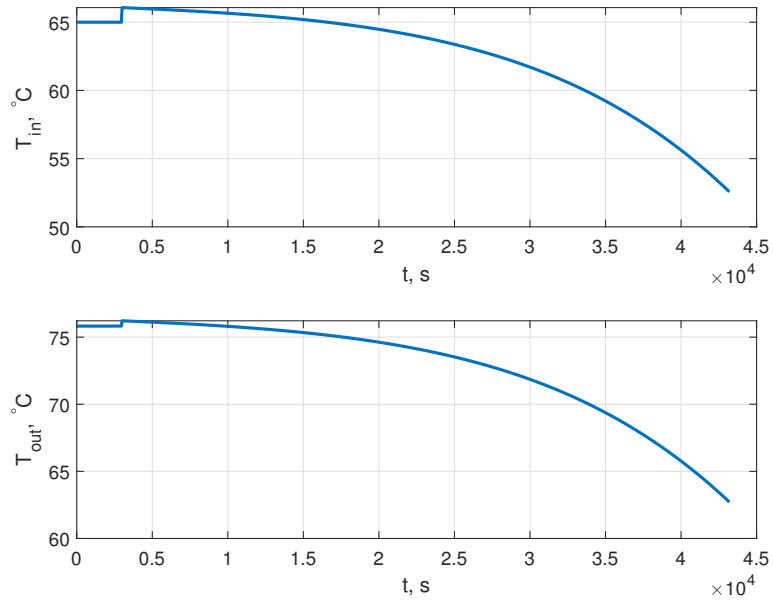

Figure 3.9: Response of inlet lye temperature T_{in} and outlet lye temperature from the electrolyzer assembly T_{out} to +20% step in the inlet lye flowrate to Electrolyzer 2

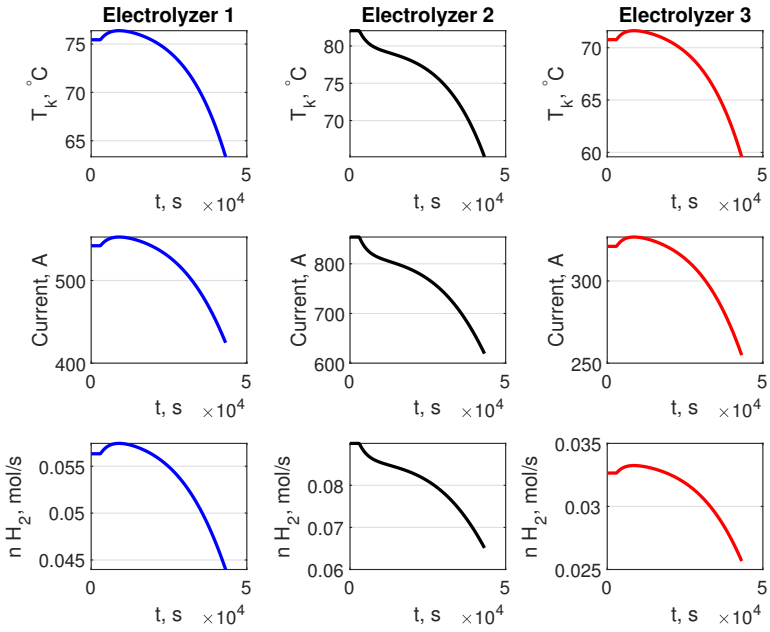

Figure 3.10: Responses to +20% step in the inlet lye flowrate to Electrolyzer 2

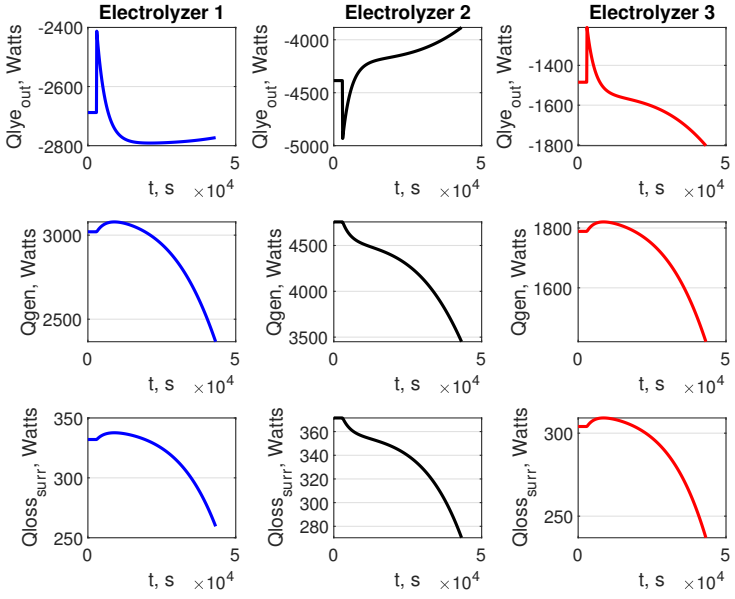

Figure 3.11: Responses of heat taken out by lye $Qlye_{out}$, heat generated inside electrolyzer $Qgen$ and heat loss in electrolyzer $Qloss_{surr}$ to +20% step in inlet lye flowrate to Electrolyzer 2

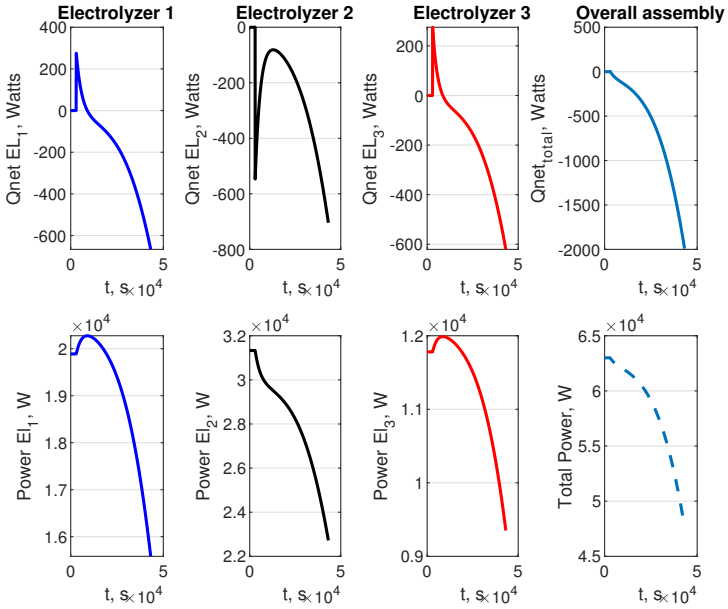

Figure 3.12: Response of total heat enthalpy and supplied power to +20% step in inlet lye flowrate to Electrolyzer 2

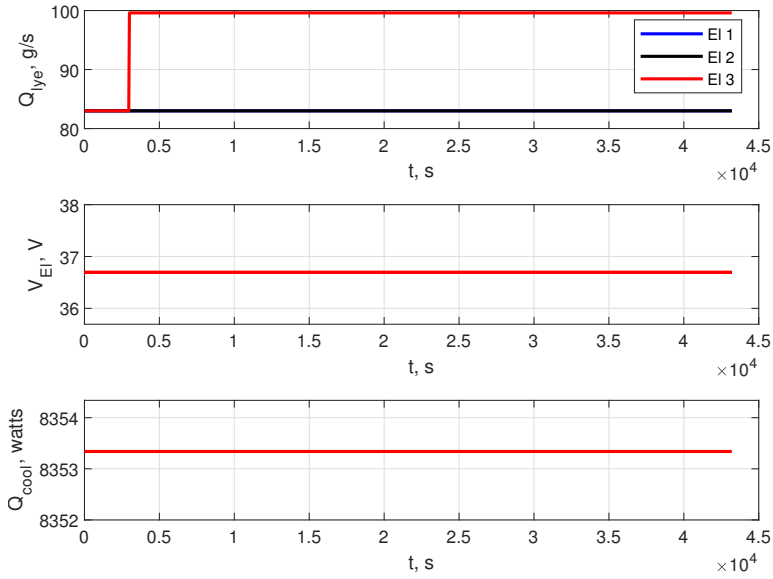

Figure 3.13: +20% step in the inlet lye flowrate to Electrolyzer 3, while cooling duty Q_{cool} and electrolyzer voltage V are kept constant

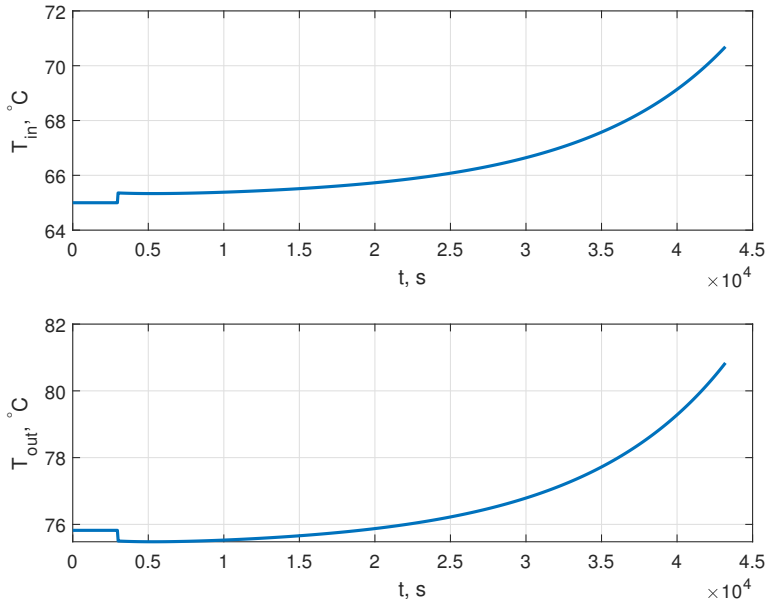

Figure 3.14: Response of inlet lye temperature T_{in} and outlet lye temperature from the electrolyzer assembly T_{out} to +20% step in the inlet lye flowrate to Electrolyzer 3

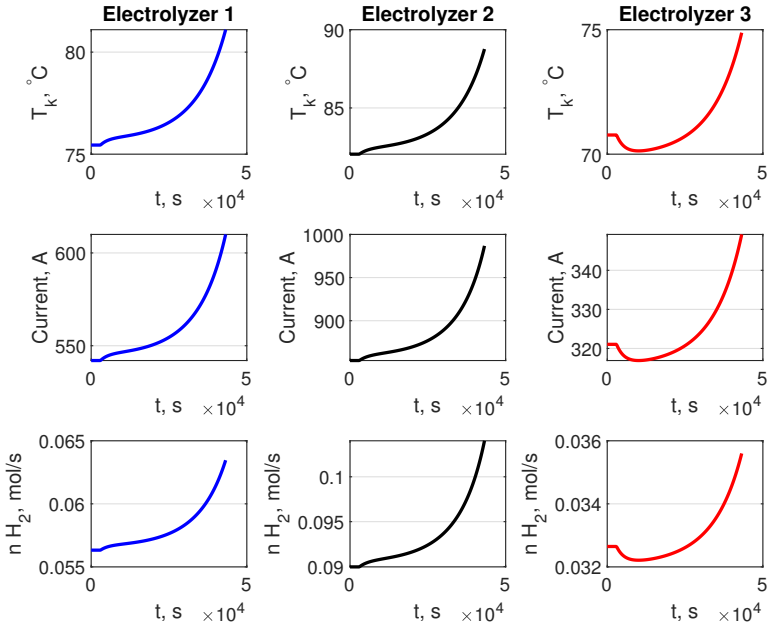

Figure 3.15: Responses to +20% step in the inlet lye flowrate to Electrolyzer 3

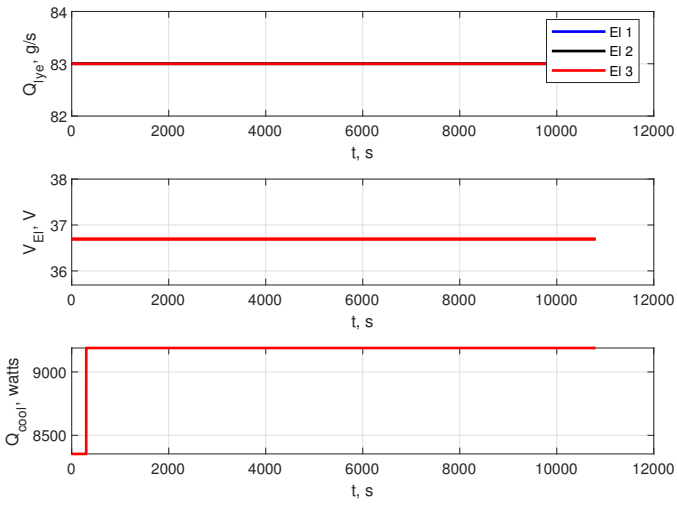

Figure 3.16: +10% step in cooling duty of the heat exchanger in the lye circulation loop

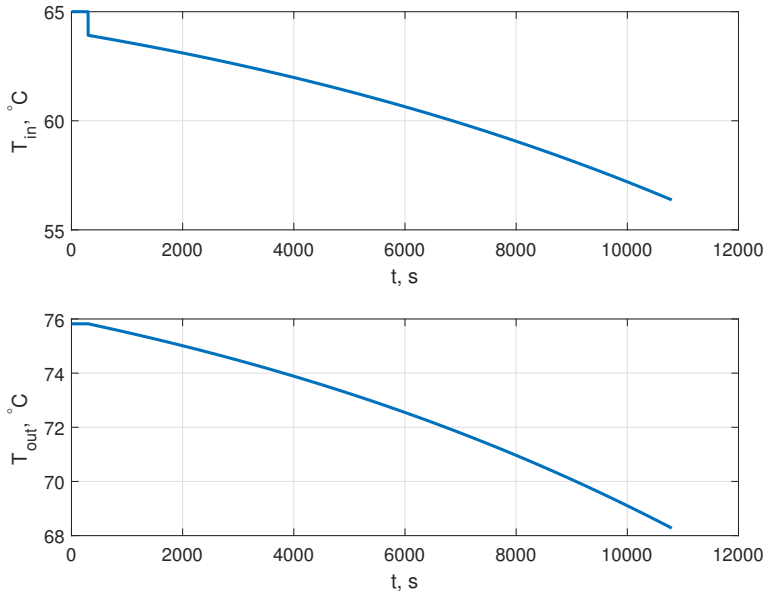

Figure 3.17: Response of inlet lye temperature T_{in} and outlet lye temperature from the electrolyzer assembly T_{out} to +10% step in cooling duty of the heat exchanger in the lye circulation loop

As expected, individual electrolyzer temperatures are also reduced in response to this change in the cooling duty and is shown in figure 3.18. Increasing cooling duty takes out more heat from the electrolyte and therefore has direct impact on the electrolyzer temperatures, inlet and outlet lye temperatures form the electrolyzer assembly. This change makes

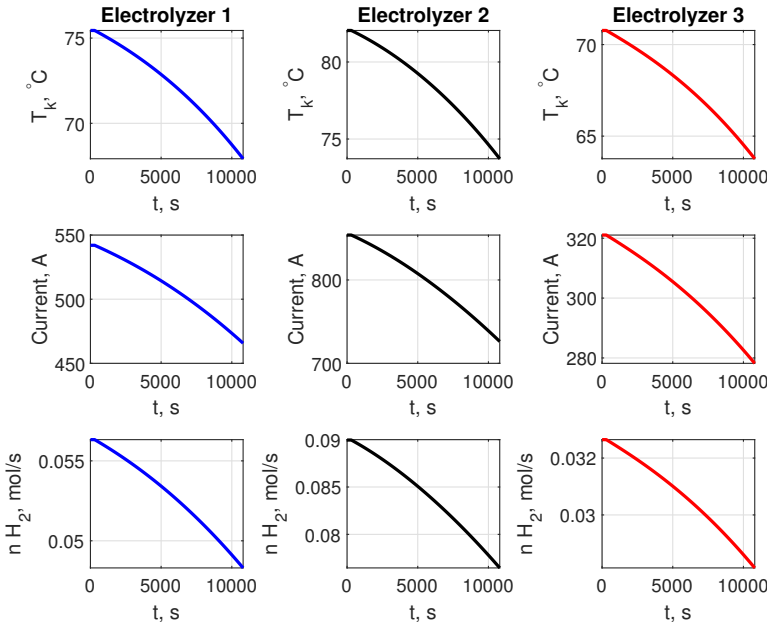

Figure 3.18: Responses to +10% step in cooling duty of the heat exchanger in the lye circulation loop

the system open loop unstable and drives it towards reduced performance profiles. Fall in the operating temperature of all three electrolyzers leads to similar decreasing trends in the electrolyzer current and hydrogen production rate (see figure 3.18). Hence, less energy is needed from power source for this reduced performance of the electrolyzer assembly.

3.3.3 Effect of step in electrolyzer voltage on open-loop system

As shown in figure 3.19 V_{El} is increased by +1% at t = 300s and the response of dependent variables to this change is analyzed for t = 3 hours.
It is to be noted that all the three electrolyzers share a common transformer and thus are operating across a common voltage. Therefore, the step change in V_{El} will change the voltage across all electrolyzer in the electrolyzer assembly. This increment in voltage will increase the power demand by each electrolyzer and subsequently the total power requirement which is shown in the figure 3.20.
Increase in power across each electrolyzer increases the electrolyzer current. Higher currents increases the electrolyzer temperature, seen in figure 3.21. This clearly suggests that the system is open loop unstable system and therefore control of electrolyzer temperature and power is needed. Higher current densities across the electrolyzer also increases the hydrogen production rate in every electrolyzer (see figure 3.21). Higher electrolyzer operation temperature increases the outlet lye temperature from the electrolyzer assembly, which is self evident and is shown in the figure 3.22.

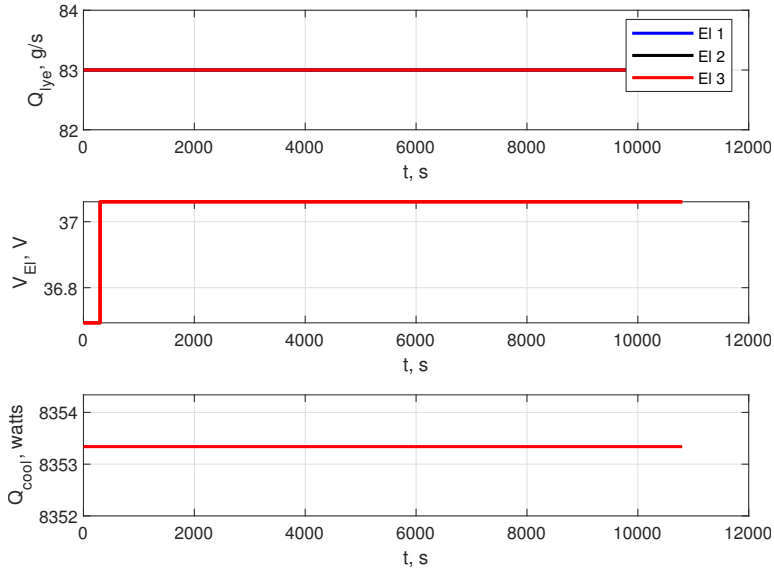

Figure 3.19: +1% step in electrolyzer voltage at t = 300s

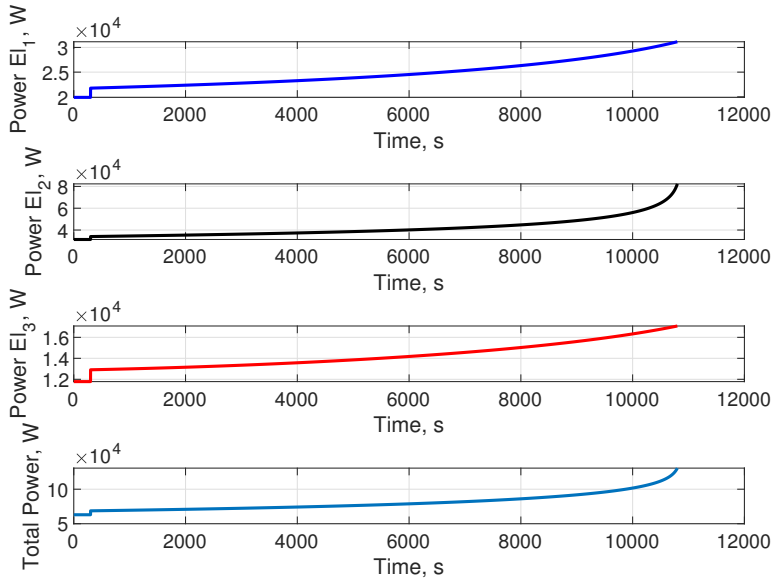

Figure 3.20: Response of electrolyzer power to +1% step in electrolyzer voltage

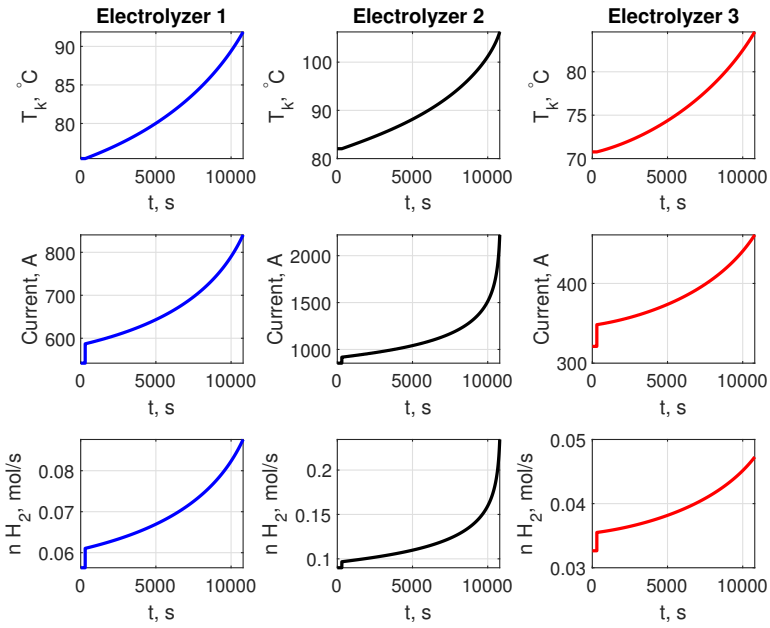

Figure 3.21: Responses to +1% step in electrolyzer voltage

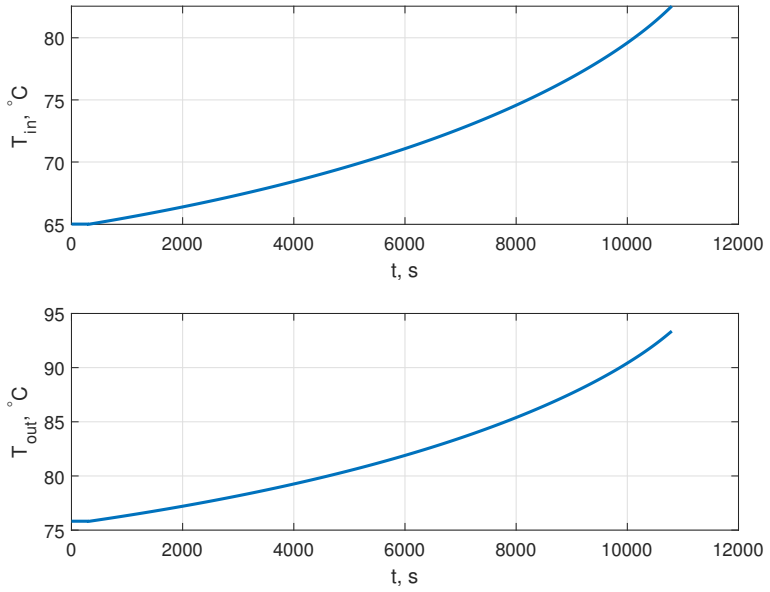

Figure 3.22: Response of inlet lye temperature T_{in} and outlet lye temperature from the electrolyzer assembly T_{out} to +1% step in electrolyzer voltage

3.3.4 Effect of step in the storage tanks outlet valve opening on open-loop system

The gas throughput from hydrogen storage tank is reduced by changing valve opening from 0.4 to 0.2 at t = 300s (see figure 3.23) and the response of dependent variables to this change is analyzed for t = 3 hours.

The figure 3.24 shows that the change in valve opening does have any impact on the

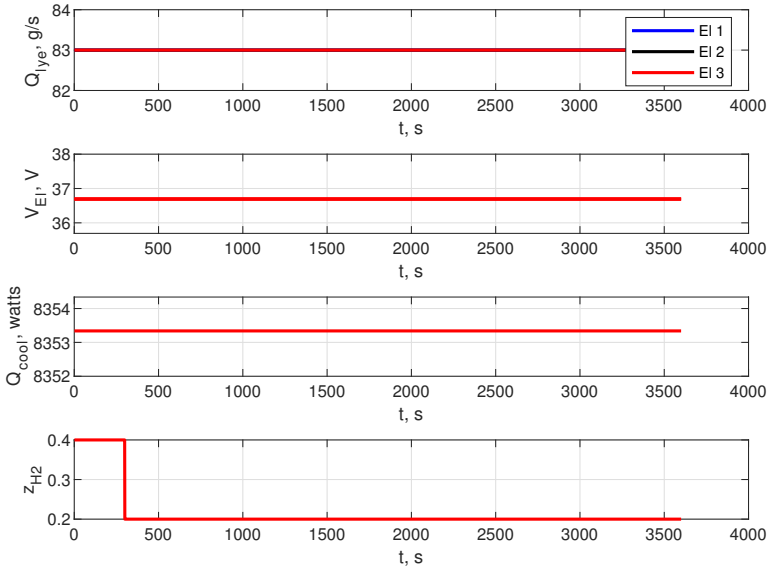

Figure 3.23: Step in outlet valve opening at t = 300s

temperatures of lye coming out (T_{out}) and lye going into (T_{in}) the electrolyzer assembly. Therefore, it is evident that the performance of electrolyzers will remain unchanged from the change in the outlet valve opening. However, change in valve opening has a direct impact on the gas storage pressure as seen from the figure 3.24. Closing the valve will increase the gas storage pressure and thereby more compressor power will be required to store gas at higher pressure.

Closing the outlet valve valve of oxygen storage tank will also have the same effect on the electrolyzer system, gas storage pressure and compressor power. Therefore, separate discussion on the effect of change in outlet valve opening of oxygen storage tank is omitted.

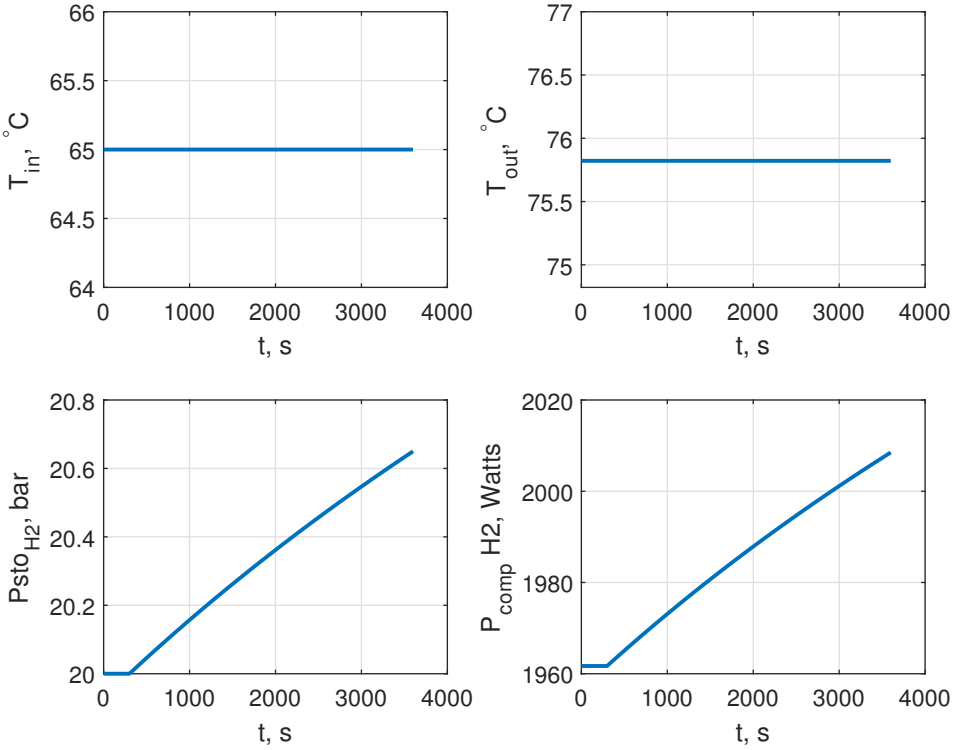

Figure 3.24: Responses to step in outlet valve opening at t = 300s

Chapter 4

Controllability analysis

This chapter explores the design of the control structures. In the previous chapter, it was observed that manipulating any available process input has an open loop positive feedback which drifts the process towards instability. In addition, simulations showed a direct relationship between the process variables like temperature, current and production rates. This suggests that having a tight control on one of the these variables makes it possible to prevent the unstable drifts in other variables as well. This argument can be validated by carrying out stability analysis of the linearized model, which is expected to reveal only one unstable pole i.e pole in the right hand complex plane (this is however not included in the scope of the current study). The dynamic step response analysis in the previous chapter formed the foundation for controllability study in this chapter.
It is highlighted from the previous chapter that the important process variables (regulatory control variables, CV_2) needs to be controlled tightly to stabilize the plant before we decide on the control of supervisory control variables CV_1. This hierarchical control structure design can be explained from the figure 4.1 and is a very common method of designing control for a typical chemical plant.

In this chapter, control structure design is done for the regulatory layer. The regulatory layer control is important to stabilize the process using low complexity controllers so that process does not drift away too far and operates close to the nominal operating point. The set-point to the regulatory layer is provided by the supervisory layer which utilizes the steady state degree of freedom and any unused manipulated variable present in the process.
Once the regulatory control layer is successfully implemented, the design of supervisory layer based on the decentralized (single-loop) control or multi-variable control (MPC) can be taken up to counteract the process disturbances or/and to improve process economics. However, this is part of further studies on this project and is therefore not discussed here.

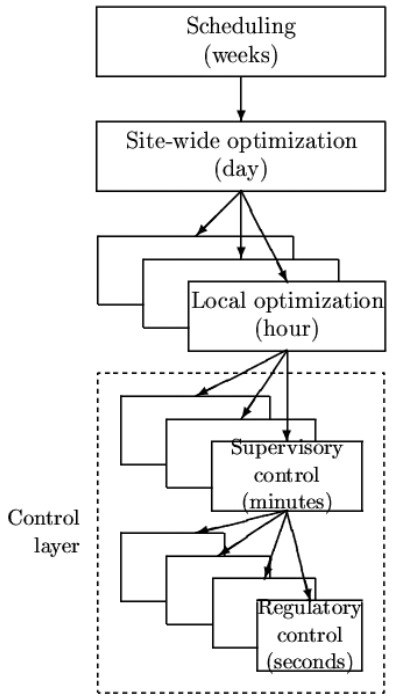

Figure 4.1: Typical control hierarchy in a chemical process plant [18]

4.1 Regulatory layer control structure

From the dynamic open loop responses observed in the previous chapter it can be concluded that the root cause of the instability is mismatch between the net heat generated and the overall heat removed from the system. The heat generated in the system is dependent on the performance of the electrolyzers, the better performance leads to higher heat generation. Hence, if Q_{cool} i.e. heat removed in lye circulation loop is kept fixed then there is net positive heat in the system (see figure 3.6) and the temperature of all electrolyzers is observed to drift to higher values in due course of time (see figure 3.5). Therefore, manipulating Q_{cool} can prove to be good idea as it directly effects the root cause of the problem. The response to +10% step in Q_{cool} are shown in figure 3.17 and 3.18. The choice of control variable (CV_2) for regulatory layer should be such that the selected CV_2 is responsive to the change in the Q_{cool} i.e. manipulated variable. We see from figure 3.17 that Q_{cool} has direct effect on T_{in} i.e. the inlet temperature of lye going into the electrolyzer. The sensitivity of T_{in} to Q_{cool} is higher than the other process variables (like T_{out} and T_k). Therefore, the process gain for transfer function from Q_{cool} to T_{in} will be higher compared to other probable candidate for a CV_2. That is why, the Q_{cool} and T_{in} are considered as an ideal MV-CV pair for regulatory layer control.
The initial response of Q_{cool} to T_{in} is approximated as a zero order process because of immediate effect on T_{in} from Q_{cool} and is controlled using a simple proportional controller.

For proportional controller, controller output $u(t)$ is proportional to the error signal, $e(t)$ = $y_{sp}(t)$ - $y_m(t)$ where, $y_{sp}(t)$ and $y_m(t)$ are the output variable set-point and measurement respectively. The controller output $u(t)$ is related to error signal $e(t)$ as,

$$u(t) = K_c \cdot \mathrm{e(t)} \tag{4.1}$$

where, K_c is the controller gain and is the tuning parameter for the proportional controller. The value of K_c is adjusted to make controller outputs as sensitive as desired to the deviations from the set value. Also, the sign of K_c is selected to make controller output increase (or decrease) as error signal increases.
From figure 3.17, we see the initial response of T_{in} to the +10% step in the Q_{cool} (see figure 3.16). The value of K_c is chosen as inverse of process gain from Q_{cool} to T_{in}, i.e.

$$K_c = -\frac{\Delta \mathrm{Q_{cool}}}{\Delta \mathrm{T_{in}}} = -774.074 \tag{4.2}$$

The choice of set point for T_{in} (i.e. 65 °C) is based on initial guess as it was the initial nominal operating point. However, while deciding the control structure for supervisory layer, T_{in} set-point (or $y_{sp}(t)$) will be an available steady state degree of freedom and it will be decided based on the design objectives for the supervisory layer.

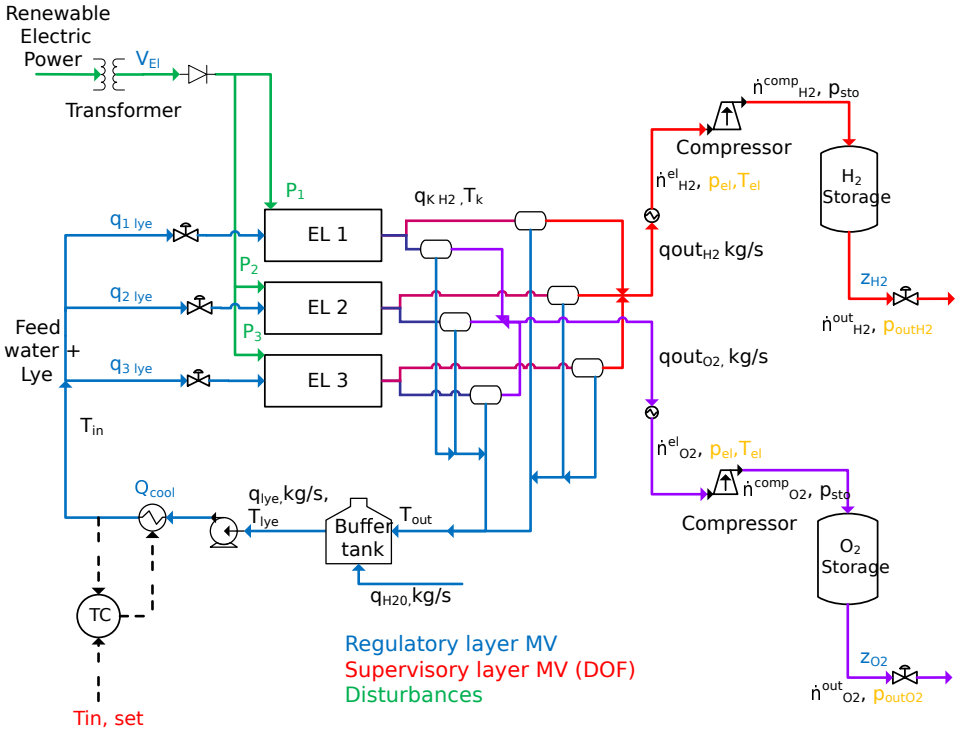

Figure 4.2: Flowsheet of alkaline water electrolyzer plant with control structure for T_{in} set-point installed

The control structure for the control of T_{in} set-point can be seen in figure 4.2. The function of this control layer is to stabilize the plant for the step changes in the supervisory layer manipulated variables (MV_1). These MV_1 are control variables for the lower regulatory layer CV_2.

4.1.1 Effect of change in the set-point for inlet lye temperature T_{in} on the controller performance

Figure 4.3 shows the change in the set-point value for inlet lye temperature from 65 °C to 66 °C at t = 7000s. Higher set-point value for T_{in} means more heat requirement i.e. less cooling in the lye circulation loop. Therefore, we see initial decrease in the cooling demand Q_{cool} (see figure 4.3). However, as we know from open loop dynamic responses in the previous chapter that increasing inlet temperature will increase the temperature of the electrolyzers (see figure 3.5) and improves the electrolyzer performance. These increasing electrolyzer temperatures have tendency of drifting away the process towards instability (see figure 3.4 and figure 3.5), which is clearly avoided after implementation of the control structure to control T_{in} (see figure 4.4). This has been possible now, because the regulatory layer is continuously manipulating Q_{cool} (see figure 4.3) to match the cooling requirement for a given set-point value of the inlet temperature T_{in}.

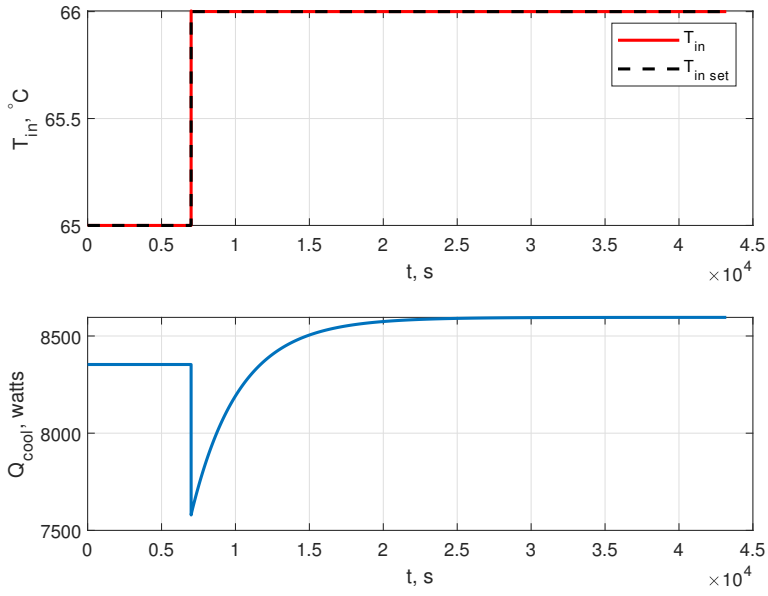

Figure 4.3: Set-point change in inlet lye temperature (CV_2) at t = 7000s from 65 °C to 66 °C. Response of Q_{cool}, i.e. MV_2 is also shown

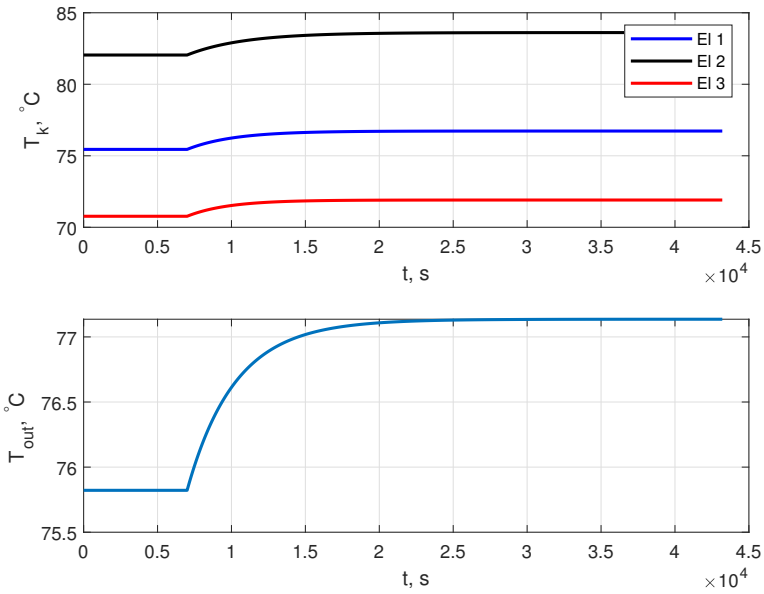

Figure 4.4: Response of temperature of electrolyzer, T_k and lye temperature at outlet, T_{out} to set-point change in T_{in}

4.1.2 Effect of disturbance in lye feed q_{1lye} on the controller performance

Figure 4.5 shows the change in the set-point value for inlet lye temperature from 65 °C to 66 °C at t = 5000s. In addition, there is also a disturbance of +20% in the inlet lye feed to electrolyzer 1 i.e. q_{1lye} at t = 10000s (see figure 4.6). The controller performance to change in set-point value and ability to reject disturbances is discussed.

Higher set-point value for T_{in} means more heat requirement i.e. less cooling in the lye circulation loop. Therefore, we see initial decrease in the cooling demand Q_{cool} (see figure 4.5). However, as we know from open loop dynamic responses in the previous chapter that increasing inlet temperature will increase the temperature of the electrolyzers and improves the electrolyzer performance. Additionally, a disturbance of +20% in the q_{1lye} will increase T_{in} (see figure 3.4), which will also have a positive effect on the electrolyzer temperature. These increasing electrolyzer temperatures have tendency of drifting away the process towards instability (see figure 3.21) which is clearly avoided because of stabilized T_{out} (see figure 4.6) after implementation of the control structure to maintain T_{in} at its set-point value. This has been possible now, because the controller is continuously manipulating Q_{cool} (see figure 4.5) to match the cooling requirement for a given set-point value of the inlet temperature T_{in}.

Also, it should be noted that the controller performance is almost ideal as it has successfully rejected the disturbance without any delay. This is because there is zero order dynamics between Q_{cool} and T_{in}, which is primarily because of the linear relationship between these variables in our model. However, this is a very ideal realization of the actual

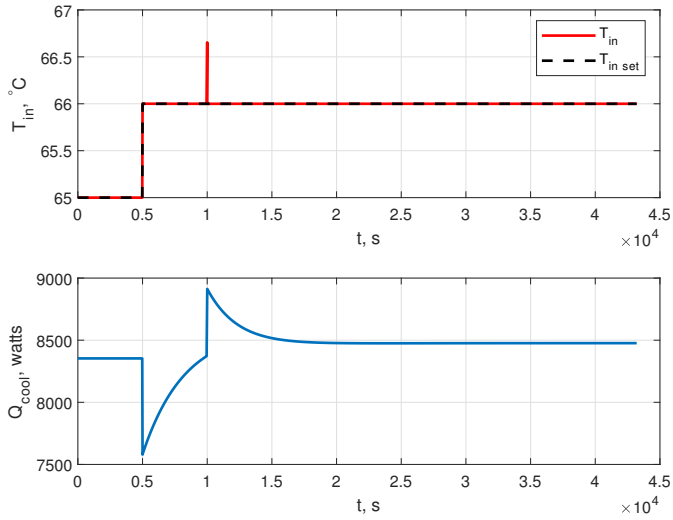

Figure 4.5: Set-point change in inlet lye temperature (CV_2) at t = 5000s from 65 °C to 66 °C. Response of Q_{cool}, i.e. MV_2 is also shown

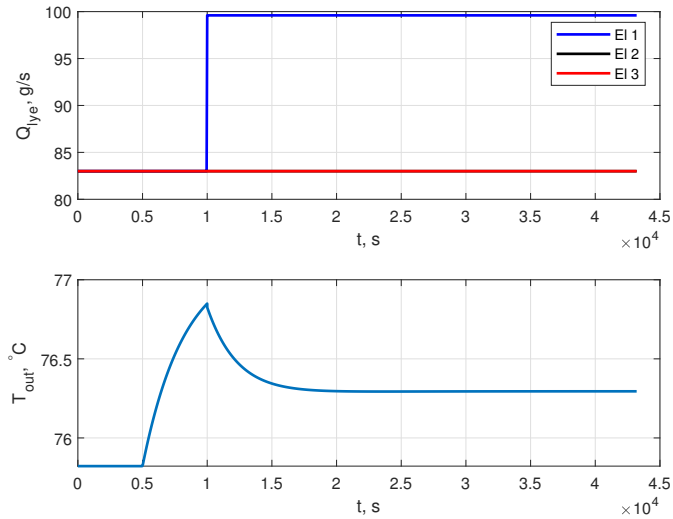

Figure 4.6: +20% disturbance in q_{1lye} at t = 10000s. Response of T_{out} with control structure for T_{in} set-point installed.

scenario and can be made more realistic by developing a heat exchanger model to relate these two variables. This is planned to be implemented in the future work on this project.

4.1.3 Proposal for regulatory layer control structure

The aim of regulatory control layer is to stabilize the plant at nominal operating point. The set-point for the controlled variables in regulatory layer (CV_2) is given by the supervisory layer on the top.
In previous section, we discussed control of only T_{in} using Q_{cool} as a manipulating variable. The rest of the control structure is shown in the figure 4.7. The MV-CV pairing suggested for remaining regulatory layer structure is as follows:

- Temperature of the each individual electrolyzer T_k is controlled using respective inlet lye flow rates q_{klye}.
- The power P_k is controlled using electrolyzer voltage, V_{El}.
- Pressure in hydrogen gas storage tank, $Psto_{H2}$ is controlled using valve opening, z_{H2}
- Pressure in oxygen gas storage tank, $Psto_{O2}$ is controlled using valve opening, z_{O2}
- Total inlet lye flowrate, q_{lye} can be also be controlled using flowrate of water added to the buffer tank, q_{H_2O}

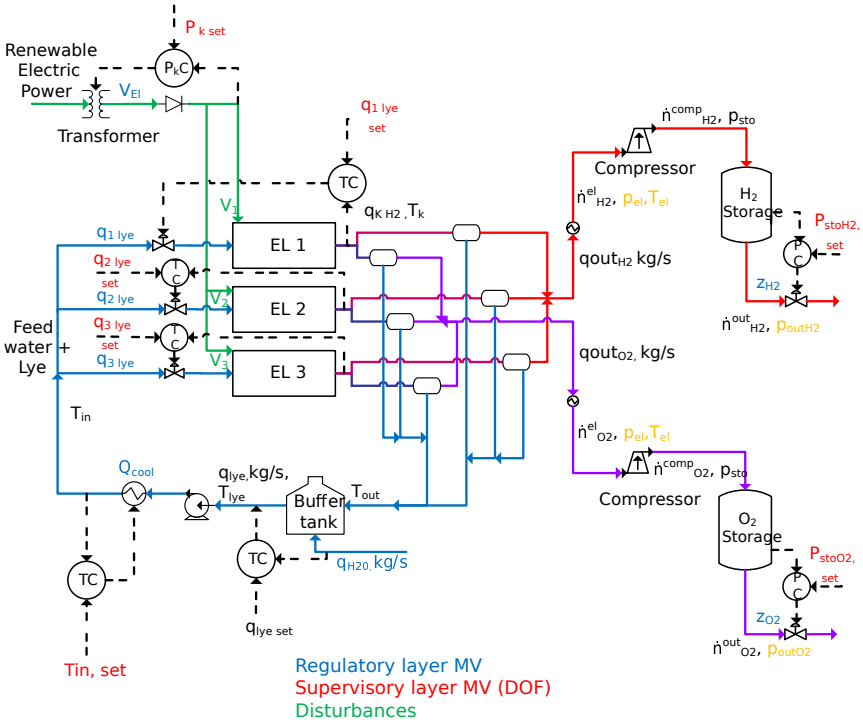

Figure 4.7: Flowsheet of alkaline water electrolyzer plant with control structure for regulatory control layer installed

The implementation and testing of this proposed regulatory control structure is not included in current work and is planned for the further work on this project.

Chapter 5

Conclusions and Recommendations

This project has developed a mathematical model of an alkaline water electrolyzer plant using systems approach. The developed model is successfully implemented in MATLAB using CasADi symbolic framework. This study has assumed usage of renewable power sources which are intermittent in nature, that is why the possible application of automatic control to ensure flexible operation is explored thereafter. Through the simulations, it was demonstrated that with the assumptions used, the model is inherently unstable because of observed open loop positive feedback that drifts the process variables towards instability. Open loop instability in the process makes it important to include a regulatory layer control structure before any further control investigations can be performed. This instability is because of mismatch between the net heat generated and total heat removed from the system. Therefore, using the cooling duty in the lye circulation loop this mismatch is eliminated by maintaining inlet lye temperature T_{in} into the electrolyzer assembly to a given set-point value. This successful implementation of temperature controller for T_{in}, which is one of the controllers in the complete scheme for regulatory control layer sets a clear path for the design of supervisory control layer. The design and testing of rest of the controllers in regulatory layer is planned to be included in future work. The supervisory control layer is expected to use all the available steady state degree of freedom present in the process to reject the disturbances in given external reference power profile and minimize the desired objective cost. The design of supervisory layer control structure is planned for future work and therefore will be investigated later.

5.1 Future work

The recommendations for the future work basically involves implementation of remaining controllers in the regulatory layer, supervisory control layer and removing certain simplifying assumptions to make process model more realistic. These are outlined below.

- This work includes controller design for inlet lye temperature T_{in} only. The design and testing of remaining controllers in the regulatory layer (see figure 4.7) will be

performed in further work on this topic.

- During the implementation of regulatory layer controller for T_{in}, the choice of inlet lye temperature set-point $T_{insetpoint}$ has been selected arbitrarily. In a more realistic scenario, the set-point for T_{in} will be provided to the regulatory layer from the supervisory layer above based on the optimized economic criterion for the chosen electrolyzer assembly. Hence, the design of supervisory layer is genuinely important and is planned for the further work on this project.

- In the present model any change in Q_{cool} has a direct effect on the T_{in} because of linear relationship between these two variables. However, to make the model more realistic, the heat exchanger model should be improved and evaluated. The present implementation shows that the process is open loop unstable which may change with a realistic process model of the heat exchanger.

- The electrolyzer model considered for this study is based on model Ulleberg's model [19]. The U-I relationship in this model is based on empirical correlations and depends only on temperature. Therefore, efforts can be made to evaluate the accuracy of the developed process model against a more detailed physical model (for eg. recently developed multi physics model [6]). This study will prove helpful to check if the dynamic responses are accurate for the propose of model.

- To keep the model simple, the compressor is assumed to be perfectly controlled in this study. This means that all the power required for the gas compression is available. In practice, the compressor will definitely have some operation limits that depends on the amount of power available for such auxiliary operations. Therefore decision on the maximum power consumption by the compressor can be included in the economic objective cost when designing the supervisory control layer in the next part of this project.

Bibliography

[1] Joel A.E. Andersson, Joris Gillis, Greg Horn, James B. Rawlings, and Moritz Diehl. CasADi: a software framework for nonlinear optimization and optimal control. *Mathematical Programming Computation*, 11(1), 2019.

[2] Cyril Bourasseau and Benjamin Guinot. Chapter 8 Hydrogen: A Storage Means for Renewable Energies. *Hydrogen Production: by Electrolysis*, 2015.

[3] Boyun Guo, Xinghui Liu, and Xuehao Tan. Chapter 11 - Transportation Systems. *Petroleum Production Engineering*, pages 275–325, 2017.

[4] Alexander Buttler and Hartmut Spliethoff. Current status of water electrolysis for energy storage, grid balancing and sector coupling via power-to-gas and power-to-liquids: A review. *Renewable and Sustainable Energy Reviews*, 82:2440–2454, 2 2018.

[5] Marisol Cervantes-Bobadilla, Ricardo Fabricio Escobar Jiménez, Jos Francisco Gmez Aguilar, Tomas Emmanuel Higareda Pliego, and Alberto Armando Alvares Gallegos. Modelling and control of an alkaline water electrolysis process. *International Journal of Computational Physics Series*, 1(2):9–14, 2 2018.

[6] M. Hammoudi, C. Henao, K. Agbossou, Y. Dubé, and M. L. Doumbia. New multi-physics approach for modelling and design of alkaline electrolyzers. *International Journal of Hydrogen Energy*, 37(19):13895–13913, 10 2012.

[7] Philipp Haug, Bjarne Kreitz, Matthias Koj, and Thomas Turek. Process modelling of an alkaline water electrolyzer. *International Journal of Hydrogen Energy*, 42(24):15689–15707, 6 2017.

[8] Christian Henao, Kodjo Agbossou, Mhamed Hammoudi, Yves Dubé, and Alben Cardenas. Simulation tool based on a physics model and an electrical analogy for an alkaline electrolyser. *Journal of Power Sources*, 250:58–67, 2014.

[9] W. Hug, H. Bussmann, and A. Brinner. Intermittent operation and operation modeling of an alkaline electrolyzer. *International Journal of Hydrogen Energy*, 18(12):973–977, 1993.

[10] International Fertilizer Association. Estimating & Reporting Fertilizer-Related Greenhouse Gas Emissions: linking Fertilizer Best Management Practices with national climate change mitigation targets. pages 1–12, 2018.

[11] Ali Keçebaş, Muhammet Kayfeci, and Mutlucan Bayat. Electrochemical hydrogen generation. *Solar Hydrogen Production*, pages 299–317, 2019.

[12] H. Kojima, T. Matsuda, H. Matsumoto, and T. Tsujimura. Development of dynamic simulator of alkaline water electrolyzer for optimizing renewable energy systems. *Journal of International Council on Electrical Engineering*, 8(1):19–24, 1 2018.

[13] Subramani Krishnan, Matthew Fairlie, Philipp Andres, Thijs de Groot, and Gert Jan Kramer. Power to gas (H2): alkaline electrolysis. *Technological Learning in the Transition to a Low-Carbon Energy System*, pages 165–187, 2020.

[14] Rodney L. LeRoy. The Thermodynamics of Aqueous Water Electrolysis. *Journal of The Electrochemical Society*, 127(9):1954, 1980.

[15] D Martinez, R Zamora, David Martinez, and Ramon Zamora. MATLAB Simscape Model of An Alkaline Electrolyser and Its Simulation with A Directly Coupled PV Module. *International Journal of Renewable Energy Research*, 8(1), 2018.

[16] Max Appl. Ammonia. In *Ullmanns encyclopedia of industrial chemistry*. 2012.

[17] Kazuo Onda, Takahiro Kyakuno, Kikuo Hattori, and Kohei Ito. Prediction of production power for high-pressure hydrogen by high-pressure water electrolysis. *Journal of Power Sources*, 132(1-2):64–70, 5 2004.

[18] Sigurd Skogestad. Control structure design : What should we control , measure and. *First African Control Conference, Cape Town*, 2003.

[19] Oystein Ulleberg. Modeling of advanced alkaline electrolyzers: a system simulation approach. *International Journal of Hydrogen Energy*, 28(1):21–33, 2003.

[20] Alfredo Ursúa, Luis M. Gandía, and Pablo Sanchis. Hydrogen production from water electrolysis: Current status and future trends. *Proceedings of the IEEE*, 100(2):410–426, 2 2012.

[21] J. P. Vanhanen and P. D. Lund. Computational approaches for improving seasonal storage systems based on hydrogen technologies. *International Journal of Hydrogen Energy*, 20(7):575–585, 1995.

[22] Tao Zhou and Bruno Francois. Modeling and control design of hydrogen production process for an active hydrogen/wind hybrid power system. *International Journal of Hydrogen Energy*, 34(1):21–30, 1 2009.

Appendix A

This chapter includes the nominal values of all the parameters used for the simulation.

Parameters for lye circulation system, gas storage and compressor

Variable	Definition	Value	Unit
Power	Total power to all electrolyzers	63000	Watts
q_{lye}	Total lye flow rate	83*N	g/s
T_{ini}	Temperature of lye at electrolyzer inlet	65	C
$Vsto_{H2}$	Volume of hydrogen storage tank	9500	litres
$Vsto_{O2}$	Volume of oxygen storage tank	4750	litres
$Pout_{H2}$	Gas outlet pressure from H_2 storage	19	bar
$Pout_{O2}$	Gas outlet pressure from O_2 storage	19	bar
$Tsto_{H2}$	Temperature of H_2 storage tank	298	Kelvin
$Tsto_{O2}$	Temperature of O_2 storage tank	298	Kelvin
T_{el}	Inlet gas temperature to the compressor	298	Kelvin
P_{el}	Inlet gas pressure to the compressor	3	bar
$VdispH_2$	Valve displacement of H_2 storage tank	0.4	
$VdispO_2$	Valve displacement of O_2 storage tank	0.4	
α	compressor efficiency	0.63	
k	polytropic efficiency	1.62	

Parameters for electrolyzers

Variable	Electrolyzer 1	Electrolyzer 2	Electrolyzer 3
r_1	$8.05 * 10^{-5}$	$6.84 * 10^{-5}$	$11.27 * 10^{-5}$
r_2	$2.5 * 10^{-7}$	$2.5 * 10^{-7}$	$2.5 * 10^{-7}$
s	0.185	0.167	0.204
t_1	-0.1002	-0.1002	-0.1002
t_2	8.424	8.424	8.424
t_3	247.3	247.3	247.3
f_1	250	225	275
f_2	0.96	0.97	0.95
C_t	625000	625000	625000
R_t	0.167	0.167	0.167

Appendix B

MATLAB code

This chapter includes MATLAB code used for implementing the developed model. The file *main.m* defines the symbolic variables. First, the DAE system developed for the model is solved at steady state with Newton rootfinder of CasADi. This is included in file *elss.m*. Next, the steady-state values are used to initialize the IDAS integrator. The input parameters can be found in the file *parElectrolyzer.m*.

main.m

```
clc
clear
close all

%% Load CasADi
%addpath('/Users/mdrizwan/Documents/MATLAB/casadi-osx-
    matlabR2015a-v3.4.5')
import casadi.*

%Using CasADi we are solving system of ODE and nonlinear
    algebraic eqns simultaneously

%Nonlinear algebraic equation are:
%1N)UI*nc-Power = 0;
%2N)U - (((r1+r2*T)*I)/A) - s*log10(((t1+(t2/T)+(t3/T^2))*I
    /A)+1) - Urev = 0;
%3N)U*nc - V = 0; U=cell voltage; V=electrolyzer voltage
%4N)Feff - ((.1*I/A)^2)/(f1+((.1*I/A)^2))*f2;
%5N)nH2el - Feff*nc*I/(ze*FC);
%6N)qH2Oloss - nH2*MwtH2O = 0;
%7)nH2elnet - sum(nH2el) = 0;
%8)nH2out - kvlvH2*VdispH2*sqrt(PstoH2-PoutH2) = 0;
%9)nO2elnet - nH2elnet/2 = 0;
%10)nO2out - kvlvO2*VdispO2*sqrt(PstoO2-PoutO2) = 0;
```

```
%11)Tout - ((sum(qlye*T)*CpLye - sum(qloss*T)*Cp + sum(
    qloss)*(Cp-CpLye)*Tref)/((sum(qlye)-sum(qloss))*Cp) = 0;
%12)Tin - Tout + Qcool/qlye*CpLye = 0;

%ODE eqautions are:
%1N)dT/dt = qlye*CpLye*(T_in-T) + nc*(U-Utn)*I - (T-Ta)/Rt)
    )/Ct;
%2)dPstoH2/dt = (TstoH2*Rg/VstoH2)*(nH2-nH2out);
%3)dPstoO2/dt = (TstoO2*Rg/VstoO2)*(nO2-nO2out);
%4)dM_bt/dt = (qlye-qloss) + qH2O - qlye;

%Parameters for the simulation are:
%1)Power
%2)qlye
%3)Qcool
%4)zH2
%5)zO2
%6)qH2O

%% Loading parameters
N = 3;                                  %no. of electrolyzers
par = parElectrolyzer(N);

%% Inputs for the simulation
Power = 21000*3;                        %power to all the
    electrolyzers, [Watts]
num_hr = 1;                             %no. of hours
t0 = 1;                                 %start, [s)]
ts = 1;                                 %time step, [s]
tf = num_hr*60*60;                      %final, [s]
tsamp = t0:ts:tf;
len = length(tsamp);                    %number of
    simulation time steps
tstep = 3000;
%% Steady state solution and calculation of valve constant
%The steady state solution is calculated by solving non
    linear algebraic equations for the steady state system
%Valve constant (k_vlv) is calculated for steady state
    condition and is kept constant for rest of the
    simulation

%initialization for steady state solution
T_ini = 65*ones(len,1);                 %assumed steady
    state temperature of the lye into the electrolyzer
T_ini(1000:end,1) = 66;
```

```
59
60 param.Ps0 = Power/N;              %initial guess for power
       input to each electrolyzer, [Watts]
61 param.u0 = 2;                     %initial guess for cell
       voltage, [V]
62 param.T0 = T_ini(1);
63
64 q_lye = N*83;                 %total lye circulated, [g/s]
65 for nEl = 1:N
66     param.q_lye(nEl) = q_lye/N; %lye through each
           electrolyzer, [g/s]
67 end
68
69 % z0s = [u_ini, i_ini, Pk, Feff_ini, nH2el_ini, qH2O_loss,
       nH2out_ini, nO2el_ini, nO2out_ini, T_out]; (7N+3)
70 % x0s = [Tk_ini, Qcool, V_ini];
71
72 [x0s,z0s] = elss(param,par);
73
74 z00=[];
75 for j=1:N
76     z00 = [z00 z0s(j) z0s(N+j) z0s(2*N+j) z0s(3*N+j) z0s(4*
           N+j) z0s(5*N+j)];    %stacking of variables for
           initialization of dynamic eqns[U I P Feff nH2in
           qH2Oloss]
77 end
78
79 nH2ss = z0s(4*N+1:5*N);       %hydrogen flow rate from kth
       electrolyzer
80 nO2ss = z0s(6*N+2:7*N+1);     %oxygen flow rate from kth
       electrolyzer
81 nH2sout = z0s(6*N+1);         %total hydrogen flowing out of
        the storage at steady state
82 nO2sout = z0s(7*N+2);         %total oxygen flowing out of
       the storage at steady state
83
84 % Calculation of valve constants
85 nH2ss = sum(nH2ss);                                %net
       hydrogen flowrate from all electrolyzers at steady state
       (sum of individual contributions), [mol/s]
86 nO2ss = sum(nO2ss);                                %net oxygen
        flowrate from all electrolyzers at steady state(sum of
       individual contributions), [mol/s]
87 kvalveH2 = nH2ss/par.Storage.VdispH2;             %valve
       constant for hydrogen outlet
```

```
88  kvalveO2 = nO2ss/par.Storage.VdispO2;              %valve
        constant for oxygen outlet
89
90  Psto_iniH2 = (nH2ss/(kvalveH2*par.Storage.VdispH2))^2 + par
        .Storage.PoutH2; %initial H2 storage pressure (
        calculated from steady state solution) [bar]
91  Psto_iniO2 = (nO2ss/(kvalveO2*par.Storage.VdispO2))^2 + par
        .Storage.PoutO2; %initial O2 storage pressure (
        calculated from steady state solution) [bar]
92  mass_bt0 = 10000;

        %mass of the liquid in the buffer tank at steady state,
        [g]
93
94  x0 = [x0s(1:N) Psto_iniH2 Psto_iniO2 mass_bt0];
                                    %initial vector for dynamic
        solution of differential variables
95  z0 = [z00 nH2ss nH2sout nO2ss nO2sout z0s(7*N+3) T_ini(1)];
                %initial vector for dynamic solution of
        algebriac variables
96
97  %defining initial value of parameters for the simualation
98  Qcool = x0s(N+1);                                %cooler duty, [J/s]
99  Vss = x0s(N+2:2*N+1);                            %voltage across
        electrolyzers, [Volts]
100 Qwater = sum(z0s(5*N+1:6*N));                     %total water lost
        during electrolysis, [grams/sec]
101
102 %% Manipulated variables
103 %these are the degree of freedoms that we will utilise to
        control the system
104
105  V_El = zeros(len,N);                             %voltage across
         the electrolyzer, [Watt], len is the length of time
         vector
106 for j = 1:N
107     V_El(1:end,j) = Vss(j)*1;                     %incremental
           step change in common voltage across all
           electrolysers
108     V_El(tstep:end,j)=Vss(j)*1.01;
109 end
110
111 qlye = zeros(len,N);                             %lye flowrate,
        [g/s]
112 for j = 1:N
```

```
113         qlye(1:end,j) = param.q_lye(j)*1;        %assumed same
                lye flowarate to all the electrolyzers
114     end
115     qlye(tstep:end,1) = param.q_lye(j)*1;
116
117     Qc = Qcool*ones(len,1);                      %cooler duty as
            a manipulated variable, [J/s]
118     Qc(tstep:end) = Qcool*1;                        %
            incremental step change in coolent duty
119
120     ZH2 = par.Storage.VdispH2*ones(len,1);       %H2 valve
            displacement as a manipulated variable
121     %ZH2(tstep:end) = .2;                          %change in H2
            valve displacement
122
123     ZO2 = par.Storage.VdispO2*ones(len,1);       %O2 valve
            displacement as a manipulated variable
124     %ZO2(tstep:end) = .7;                          %change in O2
            valve displacement
125
126     qH2O = Qwater*ones(len,1);                   %flow rate of
            water added to buffer tank as a manipulated variable, [g
            /s]
127     %qH2O(tstep:end)=Qwater*1.2;                   %incremental
            step change in the water flow rate
128
129     %% Initialize plotting variables
130     Temp = zeros(len+1,N);                       %temp of the
            electrolyzer, [C]
131     Temp(1,:) = full(T_ini(1));
132
133     PstoH2 = zeros(len+1,1);                     %H2 storage
            pressure, [bar]
134     PstoH2(1) = full(Psto_iniH2);
135
136     PstoO2 = zeros(len+1,1);                     %O2 storage
            pressure, [bar]
137     PstoO2(1) = full(Psto_iniO2);
138
139     U = zeros(len,1);                            %voltage/cell in
            each of the electrolyzer, [V]
140     I = zeros(len,1);                            %current in each
            electrolyzer, [A]
141     P = zeros(len,1);
```

```
142 I_den = zeros(len,1);                    %current density in
      the electrolyzer, [A/m^2]
143 nH2in = zeros(len,1);                    %net hydrogen flow
    rate in to the storage, [mol/s]
144 nH2out = zeros(len,1);                   %net hydrogen
    flowrate out from the storage, [mol/s]
145 nH2elout = zeros(len,1);                 %hydrogen flowrate
    from each of the individual electrolyzer, [mol/s]
146 nO2in = zeros(len,1);                    %net oxygen flow
    rate in to the storage, [mol/s]
147 nO2out = zeros(len,1);                   %net oxygen
    flowrate out from the storage, [mol/s]
148 Tout = zeros(len,1);
149 Tin = zeros(len,1);
150 level = zeros(len,1);
151 SpecEl = zeros(len,1);
152 PcompH2 = zeros(len,1);                  %compressor power
    for hydrogen, [watts]
153 PcompO2 = zeros(len,1);                  %compressor power
    for oxygen, [watts]
154 Qloss = zeros(len,1);                    %heat loss to
    surrounding in the electrolyzer, [watts]
155 Qgen = zeros(len,1);                     %heat generated in
    the electrolyzer, [watts]
156 Qlosslye = zeros(len,1);                %heat taken out by
    the lye from the electrolyzer, [watts]
157 nH2inSto = zeros(len,1);                %net hydrogen
    flowrate into the storage at all timestamps, [Nm3/h]
158 P_net = zeros(len,1);                   %net power to the
    electrolyzer assembly, [watts]
159
160 %% Solving for T_el,U,I,Feff,nH2,nO2,Tout,Tin and P_sto and
      V_bt
161
162 %differential variables: T=x(1:N);PstoH2=x(N+1);PstoO2=x(N
    +2);V_bt=x(N+3)
163 %algebraic varibales: %U=z(6j-5);I=z(6j-4);P=z(6j-3);Feff=z
    (6j-2);nH2=z(6j-1);qH2Oloss=z(6j);nH2net=z(6N+1);nH2out=
    z(6N+2);nO2net=z(6N+3);nO2out=z(6N+4);
164 %Tout=z(6N+5);Tin=z(6N+6)
165 %parameters: V_El=p(1:N);qlye_k=p(N+1:2N);Qc=p(2*N+1);zH2=p
    (2*N+2);zO2=p(2*N+3);qH2O=p(2*N+4)
166
167 eqnAlg = SX.zeros(6*N+6,1);
168 eqnDiff = SX.zeros(N+3,1);
```

```
169 z = SX.sym('z',6*N+6); x = SX.sym('x',N+3); p = SX.sym('p'
    ,2*N+4);
170 %standard casadi notation, z: algebraic variable, x:
    differential variable,
171 %p: parameters (MV)
172
173
174
175 for j = 1:N
176
177     %T=x(1:N);PstoH2=x(N+1);PstoO2=x(N+2);V_bt=x(N+3)
178     %U=z(6j-5);I=z(6j-4);P=z(6j-3);Feff=z(6j-2);nH2=z(6j-1)
        ;qH2Oloss=z(6j);nH2net=z(6N+1);nH2out=z(6N+2);nO2net
        =z(6N+3);nO2out=z(6N+4);
179     %Tout=z(6N+5);Tin=z(6N+6)
180     %V_El=p(1:N);qlye_k=p(N+1:2N);Qc=p(2*N+1);zH2=p(2*N+2);
        zO2=p(2*N+3);qH2O=p(2*N+4)
181
182     %system of algebraic equations for an electrolyzer
183     eqnAlg(6*j-5) = z(6*j-5)*z(6*j-4)*par.EL(j).nc - z(6*j
        -3);

        %power = nc*UI
184     eqnAlg(6*j-4) = z(6*j-5) - (par.U(j).r1+par.U(j).r2*x(j
        ))*z(6*j-4)/par.EL(j).A - par.U(j).s*log10(((par.U(j
        ).t1+par.U(j).t2/x(j)+...
185      par.U(j).t3/x(j)^2)*z(6*j-4)/par.EL(j).A)+1) - par.
            EL(j).Urev;

            %U-I relationship
186     eqnAlg(6*j-3) = z(6*j-5)*par.EL(j).nc - p(j);

        %U(j).nc(j)=V
187     eqnAlg(6*j-2) = z(6*j-2) - ((.1*z(6*j-4)/par.EL(j).A)
        ^2)/(par.U(j).f1+((.1*z(6*j-4)/par.EL(j).A)^2))*par.
        U(j).f2;      %faraday efficiency
188     eqnAlg(6*j-1) = z(6*j-1) - z(6*j-2)*par.EL(j).nc*z(6*j
        -4)/(par.Const.ze*par.Const.FC);
                                          %nH2, H2 production
        rate from individual electrolyzer
189     eqnAlg(6*j) = z(6*j) - z(6*j-1)*par.Const.Mwt;

        %flowrate of water lost, [g/s]
190 end
191
```

```
192 sum_H2net = SX.zeros(1,1);
193 netqlye = SX.zeros(1,1);
194 netqloss = SX.zeros(1,1);
195 qlyeT = SX.zeros(1,1);
196 qlossT = SX.zeros(1,1);
197
198 for j = 1:N
199     sum_H2net = sum_H2net + z(6*j-1);        %sum of
        hydrogen from all individual electrolyzers
200     netqlye = netqlye + p(N+j);              %sum the lye
        flowing into all individual electrolyzers
201     netqloss = netqloss + z(6*j);            %sum of water
        lost from all individual electrolyzers
202     qlyeT = qlyeT+p(N+j)*x(j);               %calculate term
         qlye(k).T(k)
203     qlossT = qlossT+z(6*j)*x(j);             %calculate term
         qH2Oloss(k).T(k)
204 end
205
206 eqnAlg(6*N+1) = z(6*N+1) - sum_H2net;
                                                  %algebraic eqn
     for net hydrogen flowrate from all the electrolyzers
207 eqnAlg(6*N+2) = z(6*N+2) - kvalveH2*p(2*N+2)*sqrt(x(N+1)-
    par.Storage.PoutH2);   %algebraic eqn for net hydrogen
    flowrate from the storage tank
208 eqnAlg(6*N+3) = z(6*N+3) - z(6*N+1)/2;
                                                  %algebraic eqn
    for net oxygen flowrate from all the electrolyzers
209 eqnAlg(6*N+4) = z(6*N+4) - kvalveO2*p(2*N+3)*sqrt(x(N+2)-
    par.Storage.PoutO2);   %algebraic eqn for net oxygen
    flowrate from the storage tank
210 eqnAlg(6*N+5) = z(6*N+5) - (((qlyeT*par.Const.CpLye) - (
    qlossT*par.Const.Cp) + netqloss*(par.Const.Cp-par.Const.
    CpLye)*par.Const.Tref)/...
211      ((netqlye-netqloss)*par.Const.CpLye));
                                                  %calculation of
         Tout
212 eqnAlg(6*N+6) = p(2*N+1) - netqlye*par.Const.CpLye*(z(6*N
    +5)-z(6*N+6));          %calculation of T_in
213
214 for j = 1:N
215     eqnDiff(j) = (p(N+j)*par.Const.CpLye*(z(6*N+6)-x(j)) +
        par.EL(j).nc*(z(6*j-5)-par.EL(j).Utn)*z(6*j-4) - ((x
        (j)-par.EL(j).Ta)/par.TherMo(j).Rt))/par.TherMo(j).
        Ct;
```

```
216     %differential eqn for the electrolyzer temperature
217 end
218
219 eqnDiff(N+1) = (par.Storage.TstoH2*par.Storage.Rg/par.
        Storage.VstoH2)*(z(6*N+1)-z(6*N+2)); %differential eqn
        for hydrogen storage pressure
220 eqnDiff(N+2) = (par.Storage.TstoO2*par.Storage.Rg/par.
        Storage.VstoO2)*(z(6*N+3)-z(6*N+4)); %differential eqn
        for oxygen storage pressure
221 eqnDiff(N+3) = (netqlye-netqloss) + p(2*N+4) - netqlye;
                                              %differential eqn
        for mass in the buffer tank, [grams i.e. pho*V]
222
223
224 dae = struct('x',x,'z',z,'p',p,'ode',eqnDiff,'alg',eqnAlg);
225 F = integrator('F', 'idas', dae);
226
227
228 for i=1:len
229     %i = timestamp
230     %j = electrolyzer sequence
231
232     r = F('x0',x0,'z0',z0,'p',[V_El(i,:) qlye(i,:) Qc(i)
            ZH2(i) ZO2(i) qH2O(i)]);
233     x0 = full(r.xf);            %updating solution as new
            initial conditions
234     z0 = full(r.zf);
235
236
237     %% Storing values in plotting variables
238
239     %calculation of compressor power
240     PcompH2(i) = full(((r.zf(6*N+1)*par.Comp.k*par.Const.R*
            par.Comp.Tel)/(par.Comp.alpha*(par.Comp.k-1)))*(((r.
            xf(N+1)/par.Comp.Pel)^((par.Comp.k-1)/par.Comp.k))
            -1));
241     PcompO2(i) = full(((r.zf(6*N+3)*par.Comp.k*par.Const.R*
            par.Comp.Tel)/(par.Comp.alpha*(par.Comp.k-1)))*(((r.
            xf(N+2)/par.Comp.Pel)^((par.Comp.k-1)/par.Comp.k))
            -1));
242     %assuming same k and Tel for O2
243
244     PstoH2(i+1) = full(r.xf(N+1));          %hydrogen
            storage pressure at all timestamps, [bar]
```

```
245     PstoO2(i+1) = full(r.xf(N+2));          %oxygen storage
            pressure at all timestamps, [bar]
246     nH2in(i) = full(r.zf(6*N+1));           %net hydrogen
            flow rate in to the storage at all timestamps, [mol/
            s]
247     nH2out(i) = full(r.zf(6*N+2));          %net hydrogen
            flowrate out from the storage at all timestamps, [
            mol/s]
248     nO2in(i) = full(r.zf(6*N+3));           %net oxygen
            flow rate in to the storage at all timestamps, [mol/
            s]
249     nO2out(i) = full(r.zf(6*N+4));          %net oxygen
            flowrate out from the storage at all timestamps, [
            mol/s]
250     Tout(i) = full(r.zf(6*N+5));            %temperature of
            lye after mixing before going to the buffer tank, [
            celsius]
251     Tin(i) = full(r.zf(6*N+6));             %temperature of
            lye going into the electrolyzer, [celsius]
252     level(i) = full(r.xf(N+3));
253
254
255
256     for j=1:N
257         U(i,j) = full(r.zf(6*j-5));             %voltage/
                cell, [V]
258         I(i,j) = full(r.zf(6*j-4));             %current, [
                A]
259         P(i,j) = full(r.zf(6*j-3));             %power, [
                Watts]
260         Temp(i+1,j)= full(r.xf(j));             %
                temperature of electrolyzers at all timestamps,
                [celsius]
261         I_den(i,j) = 0.1*I(i,j)/par.EL(j).A;    %current
                density, [mA/cm^2]
262         nH2elout(i,j) = full(r.zf(6*j-1));      %hydrogen
                production rate from individual electrolyzer, [
                mol/s]
263         SpecEl(i,j) = (P(i,j)*(10^-6))./(nH2elout(i,j)*par.
                Const.MwtH2*(10^-6)*3600);   %specific
                electricity, [MWh/tonne H2]
264         Qloss(i,j) = (Temp(i+1,j) - par.EL(j).Ta)/par.
                TherMo(j).Rt;                        %heat loss to
                surrounding in the electrolyzer, [watts]
```

```
265         Qgen(i,j) = par.EL(j).nc*(U(i,j)-par.EL(j).Utn)*I(i
                ,j);                        %heat generated in
                the electrolyzer, [watts]
266         Qlosslye(i,j) = qlye(i,j)*par.Const.CpLye*(Tin(i)-
                Temp(i+1,j));               %heat taken out by
                 the lye from the electrolyzer, [watts]
267     end
268
269     nH2inSto(i) = (nH2in(i)*0.0224136*3600); %net hydrogen
            flowrate into the storage at all timestamps, [Nm3/h]
270     P_net(i)=sum(P(i,:));
271
272
273     if rem(i,1000)==0
274     disp(i)
275     end
276
277     %proportional controller for zero order process
278     %if i >= tstep
279     Qc(i+1) = Qc(i)+(836/1.08)*(Tin(i)-T_ini(i));
280     %end
281 end
282
283 %% Plotting the results
284 figure()
285 plot(I)
286 xlabel('Time, s')
287 ylabel('Current, A')
288 legend('El 1','El 2', 'El 3')
289 grid on
290
291 figure()
292 plot(U)
293 xlabel('Time, s')
294 ylabel('Cell voltage, V/cell')
295 legend('El 1','El 2', 'El 3')
296 grid on
297
298 figure()
299 subplot(1,4,1)
300 plot(P(:,1),'b')
301 xlabel('Time, s')
302 ylabel('P_1, Watts')
303 grid on
304 subplot(1,4,2)
```

```
plot(P(:,2),'k')
xlabel('Time, s')
ylabel('P_2, Watts')
grid on
subplot(1,4,3)
plot(P(:,3),'r')
xlabel('Time, s')
ylabel('P_3, Watts')
grid on
subplot(1,4,4)
plot(P_net)
xlabel('Time, s')
ylabel('Power, Watts')
grid on

figure()
plot(nH2elout)
hold on
plot(nH2in)
xlabel('Time, s')
ylabel('H_2 production rate, mol/s')
legend('El 1','El 2', 'El 3','H_2_n_e_t El')
grid on

figure()
subplot(2,1,1)
plot(PstoH2)
xlabel('Time, s')
ylabel('H_2 Storage pressure, bar')
grid on
subplot(2,1,2)
plot(PcompH2)
xlabel('Time, s')
ylabel('H_2 compressor power, watts')
grid on

figure()
subplot(3,1,1)
plot(Temp(2:end,1))
xlabel('Time, s')
ylabel('T_1, C')
grid on

subplot(3,1,2)
plot(Temp(2:end,2))
```

```
xlabel('Time, s')
ylabel('T_2, C')
grid on

subplot(3,1,3)
plot(Temp(2:end,3))
xlabel('Time, s')
ylabel('T_3, C')
grid on

figure()

subplot(2,1,1)
plot(Tout)
xlabel('Time, s')
ylabel('T_o_u_t, C')
grid on

subplot(2,1,2)
plot(Tin)
xlabel('Time, s')
ylabel('T_i_n, C')
grid on

%plot of the step in MV

figure()
%plot(V_El)
plot(Qc)
xlabel('Time, s')
ylabel('Q_c_o_o_l')
grid on
%legend('El 1','El 2', 'El 3')

%%
save('data_DVVstep3000_MVQcool_Tinset_12hr')
%%
%load data_q1step3000_MVQcool_12hr
```

elss.m

```
function [x0,z0] = elss(param,par)

%This function file solves the steady state solution for
    the system of electrolyzers
%Here we will assume inlet lye temp into electrolyzer is 80
```

```
    C at steady state
%Power, qlye and V (electrolyzer voltage) are provided as
    inputs to solve for steady state

%nEl = sequence of the electrolyzer

%Here we are solving following eqns for each electrolyzer:
%1N)UI*nc-Power = 0;
%2N)U - (((r1+r2*T)*I)/A) - s*log10(((t1+(t2/T)+(t3/T^2))*I
    /A)+1) - Urev = 0;
%3N)U*nc - V = 0; U=cell voltage; V=electrolyzer voltage
%4N)qlye*CpLye*(T_in-T) + nc*(U-Utn)*I - (1/Rt)*(T-Ta);

%% Load CasADi
%addpath('/Users/mdrizwan/Documents/MATLAB/casadi-osx-
    matlabR2015a-v3.4.5')
import casadi.*

%% Define symbolic variables
x = SX.sym('x',4*par.N);            %symbolic variables for
    cell voltage, current and electrolyzer voltage (V)
eqn = SX.zeros(4*par.N,1);
u=[];
i=[];
T_k=[];
Ps=[];


for nEl = 1:par.N
    u = [u x(nEl)];                 %cell voltage of the
        electrolyzer
    i = [i x(par.N+nEl)];           %current in the
        electrolyzer
    T_k = [T_k x(2*par.N+nEl)];     %temperature of the
        individual electrolyzer
    Ps = [Ps x(3*par.N+nEl)];       %power of the
        individual electrolyzer
end

%% Initial conditions for steady state calculations


T_in = param.T0;                                        %
    steady state temperature of lye into electrolyzer

```

```
40 u0 = zeros(1,par.N);
41 i0 = zeros(1,par.N);
42 Ps0 = zeros(1,par.N);
43 T_k0 = zeros(1,par.N);
44
45 q_lye0 = zeros(1,par.N);
46
47 for nEl = 1:par.N
48     u0(nEl) = param.u0*21/par.EL(nEl).nc;
                                %initial guess for cell
       voltage
49     Ps0(nEl) = param.Ps0;
50     q_lye0(nEl) = param.q_lye(nEl);
51     i0(nEl) = Ps0(nEl)/(par.EL(nEl).nc*u0(nEl));
                        %initial guess for current
52     T_k0(nEl) = ((q_lye0(nEl)*par.Const.CpLye*T_in) + par.
       EL(nEl).Ta/par.TherMo(nEl).Rt + ...
53         par.EL(nEl).nc*(u0(nEl)-par.EL(nEl).Utn)*i0(nEl))
           /(1/par.TherMo(nEl).Rt+q_lye0(nEl)*par.Const.
           CpLye);
54
55 end
56
57 X0 = [u0 i0 T_k0 Ps0];
58
59 %% Solving steady state problem
60 for nEl = 1:par.N
61     eqn(nEl) = u(nEl)*i(nEl)*par.EL(nEl).nc-Ps(nEl);
                                  %power = nc*UI
62     eqn(par.N+nEl) = u(nEl) - (par.U(nEl).r1+par.U(nEl).r2*
       T_k(nEl))*i(nEl)/par.EL(nEl).A - par.U(nEl).s*log10
       (((par.U(nEl).t1+par.U(nEl).t2/T_k(nEl)+...
63         par.U(nEl).t3/(T_k(nEl)^2))*i(nEl)/par.EL(nEl).A)
           +1) - par.EL(nEl).Urev;
                                                        %U-
           I relationship
64     eqn(2*par.N+nEl) = q_lye0(nEl)*par.Const.CpLye*(T_in-
       T_k(nEl)) + par.EL(nEl).nc*(u(nEl)-par.EL(nEl).Utn)*
       i(nEl) - ...
65         (1/par.TherMo(nEl).Rt)*(T_k(nEl)-par.EL(nEl).Ta);
                                    %temperature of each
           electrolyzer
66 end
67 for nEl = 1:(par.N-1)
68     eqn(3*par.N+nEl) = u(nEl)*par.EL(nEl).nc - u(nEl+1)*par
```

```
        .EL(nEl+1).nc;                                          %U(j).
        nc(j)= V
end

sumPs = SX.zeros(1,1);
for nEl = 1:par.N
   sumPs =  sumPs + Ps(nEl);
end

eqn(4*par.N) = sumPs - sum(Ps0);
                                                % V = voltage across
    last electrolyzer


g = Function('g',{x},{eqn});
G = rootfinder('G','newton',g);
res = full(G(X0));

U = [];
I = [];
T = [];
Pk = [];
for nEl = 1:par.N
    U = [U res(nEl)];
    I = [I res(par.N+nEl)];
    T = [T res(2*par.N+nEl)];
    Pk = [Pk res(3*par.N+nEl)];
end



%% Residuals check
%
%  for nEl=1:par.N
%  eq1(nEl) = I(nEl)*U(nEl)*par.EL(nEl).nc-Pk(nEl);
%  eq2(nEl) = q_lye0(nEl)*par.Const.CpLye*(T_in-T(nEl)) +
    par.EL(nEl).nc*(U(nEl)-par.EL(nEl).Utn)*I(nEl) - ...
%           (1/par.TherMo(nEl).Rt)*(T(nEl)-par.EL(nEl).Ta);
%  eq3(nEl) = U(nEl) - (par.U(nEl).r1+par.U(nEl).r2*T(nEl))
    *I(nEl)/par.EL(nEl).A - par.U(nEl).s*log10(((par.U(nEl).
    t1+par.U(nEl).t2/T(nEl)+...
%           par.U(nEl).t3/(T(nEl)^2))*I(nEl)/par.EL(nEl).A)
    +1) - par.EL(nEl).Urev;
%  end

```

```
106 %% Calculation of initial state vector
107 Feff = zeros(1,par.N);
108 nH2 = zeros(1,par.N);
109 qH2O_loss = zeros(1,par.N);
110 for nEl = 1:par.N
111     Feff(nEl)= ((0.1*I(nEl)/par.EL(nEl).A)^2)/(par.U(nEl).
        f1+((0.1*I(nEl)/par.EL(nEl).A)^2))*par.U(nEl).f2;
112     nH2(nEl) = Feff(nEl)*par.EL(nEl).nc*I(nEl)/(par.Const.
        ze*par.Const.FC);
113     qH2O_loss(nEl) = nH2(nEl)*par.Const.Mwt;
114 end
115
116 u_ini = U;
117 i_ini = I;
118 Tk_ini = T;
119 for nEl = 1:par.N
120     V_ini(nEl) = U(nEl)*(par.EL(nEl).nc);
121 end
122 Feff_ini = Feff;
123 nH2el_ini = nH2;
124 nH2out_ini = sum(nH2);
125 nO2 = nH2/2;
126 nO2el_ini = nO2;
127 nO2out_ini = sum(nO2);
128 T_out = ((q_lye0*T')*par.Const.CpLye - (qH2O_loss*T')*par.
    Const.Cp + sum(qH2O_loss)*(par.Const.Cp-par.Const.CpLye)
    *par.Const.Tref)/...
129     ((sum(q_lye0) - sum(qH2O_loss))*par.Const.CpLye); %
        temp after mixing of liquid streams from all
        electrolyzers
130 Qcool = sum(q_lye0)*par.Const.CpLye*(T_out - T_in);
                                    %cooler duty at steady
    state, [J/s]
131 kgH2 = nH2el_ini*par.Const.MwtH2*(10^-6)*3600;
132 SpecEl_ini = (Pk*(10^-6))./kgH2;
133 % for i=1:N
134 % Qgen(i) = nc(i)*(U(i)-Utn(i))*I(i)
135 % end
136
137 z0 = [u_ini, i_ini, Pk, Feff_ini, nH2el_ini, qH2O_loss,
    nH2out_ini, nO2el_ini, nO2out_ini T_out];
138 x0 = [Tk_ini, Qcool, V_ini];
139
140 % z0s = [u_ini, i_ini, Pk, Feff_ini, nH2el_ini, qH2O_loss,
    nH2out_ini, nO2el_ini, nO2out_ini, T_out]; (7N+3)
```

```
141 % x0s = [Tk_ini, Qcool, V_ini];
142
143 end
```

parElectrolyzer.m

```
1  function par = parElectrolyzer(N)
2
3  %This script defines values of the input parameters for all
       electrolyzers.
4
5  par.Const = struct('ze',2,'FC',96485,'R',8.314,'Cp',4.18,'
       CpLye',3.1,'Mwt',18,'MwtH2',2.01588,'Tref',25);%Cp=
       specific heat of water, [J/gK];Mwt=mol. wt of H2O
6  par.Comp = struct('alpha',0.63,'k',1.62,'Tel',25+273,'Pel'
       ,3);
7  par.Storage = struct('VstoH2',9500,'VstoO2',4750,'PoutH2'
       ,19,'PoutO2',19,'TstoH2',25+273,'TstoO2',25+273,'Rg'
       ,8.314e-2,'VdispH2',0.4,'VdispO2',.4);
8
9  %% Parameters for U-I relationship in Ulleberg's model
10 par.U = struct([]);
11 par.TherMo = struct([]);
12 par.EL = struct([]);
13 for i =1:N
14     par.U(i).r1 = 8.05e-5;                    %ohm m^2
15     par.U(i).r2 = -2.5e-7;                    %ohm m^2 C^-1
16     par.U(i).s = .185;                        %Vs
17     par.U(i).t1 = -.1002;                     %A^-1 m^2
18     par.U(i).t2 = 8.424;                      %A^-1 m^2 C^-1
19     par.U(i).t3 = 247.3;                      %A^-1 m^2 C^-2
20     par.U(i).f1 = 250;                        %mA^2 cm^-4
21     par.U(i).f2 = 0.96;                       %dimensionless
22
23     %% Parameters for Ulleberg's thermal model
24     par.TherMo(i).Ccw = 0.7e3;
                                                 %thermal
           capacity of cooling water, J s^-1 C^-1
25     par.TherMo(i).Ct = 625e3;        %625e3
                                 %thermal capacity of
           electrolyzer, J C^-1
26     par.TherMo(i).tauT = par.TherMo(i).Ccw*par.TherMo(i).Ct
           ;        %thermal time constant, Rt*Ct, [s]
27     par.TherMo(i).Rt = .167;
                                                   %C W^-1
28     par.TherMo(i).Tcwi = 14.5;
```

```
                                                    %inlet water
        temp, [C]
29      par.TherMo(i).hcond = 7;
                                                      %W C^-1
30      par.TherMo(i).hconv = 0.02;
                                                    %W C^-1 per A
31
32      %% Parameters for Faraday effeciency calculations
33      par.EL(i).Utn = 1.482;                      %thermoneutral
            voltage, [V]
34      par.EL(i).Urev = 1.229;                     %reversible cell
            voltage, [V]
35      par.EL(i).nc = 21;                          %no. of cells
36      par.EL(i).A = .25;                          %electrode area of
             each cell, [m^2]
37      par.EL(i).Ta = 20;                          %ambient temp, [C]
38      par.EL(i).Tstd = 25;                        %standard
            temperature, [C]
39  end
40  %El #2
41  par.U(2).r1 = 8.05e-5*0.85;                      %ohm m^2
42  par.U(2).s = .185*0.9;                          %V
43  par.U(2).f1 = 250*0.9;                          %mA^2 cm^-4
44  par.U(2).f2 = 0.97;
45
46  %El #3
47  par.U(3).r1 = 8.05e-5*1.4;                      %ohm m^2
48  par.U(3).s = .185*1.1;                          %V
49  par.U(3).f1 = 250*1.1;                          %mA^2 cm^-4
50  par.U(3).f2 = 0.95;
51
52  par.N=N;
53  end
```